

Synthesis and Characterization of Ir(III) metallacycles Derived From Thiophene and Related Compounds: Models for the Hydrodesulfurization Process

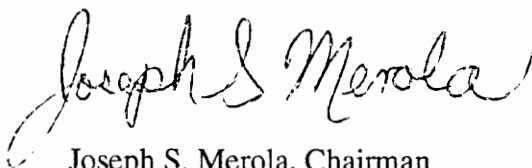
By
Arthur L. Grieb

Thesis submitted to the Faculty of the
Virginia Polytechnic Institute and State University
in partial fulfillment of the requirements for the degree of

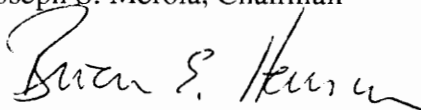
Master of Science

in

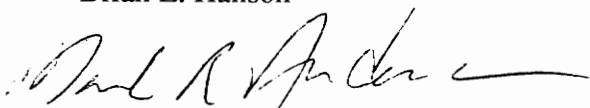
Chemistry
APPROVED



Joseph S. Merola, Chairman



Brian E. Hanson



Mark R. Anderson

August, 1993
Blacksburg, Virginia

C.2

LD
5655
V855
1993
G.753
C.2

Synthesis and Characterization of Ir(III) metallacycles Derived From Thiophene and Related Compounds: Models for the Hydrodesulfurization Process

By
Arthur L. Grieb
Joseph S. Merola, Committee Chairman
Department of Chemistry
(ABSTRACT)

Researchers use metal-thiophene complexes to mimic reactions which occur inside hydrodesulfurization (HDS) reactors. Information obtained from these model studies may often be applied to understanding the mechanisms involved with commercially used catalysts. Certain mechanisms¹ for HDS propose thiophene ring cleavage, forming a metallacycle, prior to hydrogenation of one double bond. There are, however, limited examples of complexes derived from C-S cleavage.^{2,3,4}

Thermal reactions of the iridium complex, $[\text{Ir}(\text{COD})(\text{PMe}_3)_3]\text{Cl}$ (COD=1,5-cyclooctadiene), with thiophene, thiazole, 4-methyl thiazole and 5-methyl thiazole yields the C-S addition metallacycles $(\text{Me}_3\text{P})_3\text{Ir}-(\text{CH}=\text{CHCH}=\text{S})\text{Cl}$ (**I**), $(\text{Me}_3\text{P})_3\text{Ir}-(\text{CH}=\text{NCH}=\text{CHS})\text{Cl}$ (**II**), $(\text{Me}_3\text{P})_3\text{Ir}-(\text{CH}=\text{NC}(\text{CH}_3)=\text{CHS})\text{Cl}$ (**III**) and $(\text{Me}_3\text{P})_3\text{Ir}-(\text{CH}=\text{NCH}=\text{C}(\text{CH}_3)\text{S})\text{Cl}$ (**IV**), respectively. These compounds were characterized using the following methods: ¹H NMR, ¹³C NMR, ³¹P NMR, elemental analysis and single crystal x-ray diffraction.

Following C-S addition to $[\text{Ir}(\text{COD})(\text{PMe}_3)_3]\text{Cl}$, nitrogen present in the thiazoles exhibit enhanced nucleophilicity. For example, compounds II - IV react with methylene chloride to form dimers: $\text{CH}_2[\text{NCR}=\text{CR}'\text{SIr}(\text{Cl})(\text{PMe}_3)_3\text{CH}]_2$. The above compounds are soluble in water and react with PF₆ salts liberating the chloride atom from the Ir center. *pK_b* measurements were recorded as well.

This thesis describes the synthesis and examination of compounds I-IV as they may model the HDS process. Compounds II-IV represent the first examples of ring-opened thiazole metallacycles with iridium.

Acknowledgments

I would like to take this time to thank Dr. Joseph Merola for his assistance regarding my unique situation as well as allowing me to enter his research group. His time and effort made it possible for me to continue my studies at Virginia Tech. I would also like to thank Dr. Brian Hanson and Dr. Mark Anderson for making themselves available for committee duties. Finally, I would like to thank all the members of Dr. Merola's group for any assistance they may have given me during my studies.

Table of Contents

Chapter 1: Introduction.....	1
Chapter 2: Discussion.....	10
Chapter 3: Reactivity.....	26
Chapter 4: Conclusions.....	29
Chapter 5: Experimental.....	31
References.....	37
Appendix: X-ray Crystallographic Data.....	39
VITA.....	55

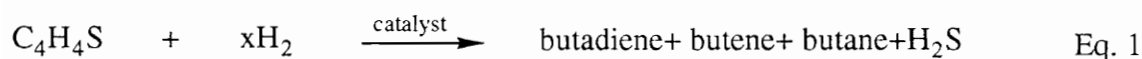
List of Illustrations

Figure 1.1 Binding modes of thiophene to metals.....	3
Figure 1.2 One-point mechanism for HDS.....	4
Figure 1.3 Multi-point mechanism for HDS.....	5
Figure 1.4 A proposed mechanism: Hydrogenation prior to C-S cleavage.....	8
Figure 1.5 Reported C-S insertion metallacycles.....	9
Figure 2.1 ORTEP of mer-(Me ₃ P) ₃ Ir{SeCHCHCH}(Cl).....	11
Figure 2.2 ¹ H NMR of mer-(Me ₃ P) ₃ Ir-(CH=NCH=CHSe)Cl.....	12
Figure 2.3 ¹³ C NMR of mer-(Me ₃ P) ₃ Ir-(CH=NCH=CHSe)Cl.....	13
Figure 2.4 Plausible isomers of ALG II.....	15
Figure 2.5 ¹ H NMR of mer-(Me ₃ P) ₃ Ir-(CH=NCH=CHS)Cl.....	16
Figure 2.6 ¹³ C NMR of mer-(Me ₃ P) ₃ Ir-(CH=NCH=CHS)Cl.....	17
Figure 2.7 Structures of new heteroaromatic metallacycles.....	18
Figure 2.8 ¹ H NMR of mer-(Me ₃ P) ₃ Ir-(CH=NC(CH ₃)=CHS)Cl.....	20
Figure 2.9 ¹³ C NMR of mer-(Me ₃ P) ₃ Ir-(CH=NC(CH ₃)=CHS)Cl.....	21
Figure 2.10 ¹ H NMR of mer-(Me ₃ P) ₃ Ir-(CH=NCH=C(CH ₃)S)Cl.....	22
Figure 2.11 ¹³ C NMR of mer-(Me ₃ P) ₃ Ir-(CH=NCH=C(CH ₃)S)Cl.....	23
Figure 2.12 Structures of related compounds for comparison.....	25
Figure 3.1 ORTEP of the dimer of ALG II.....	26
Figure 3.2 Structures of nitrogen substituted complexes.....	27
Figure 3.3 pK _b titration curve.....	28

Chapter 1: Introduction

Hydrodesulfurization (HDS) of petroleum-based feedstocks is an important commercial process (24 million barrels of petroleum processed per day worldwide in 1981).⁵ Removal of sulfur from feedstocks is necessary to avoid catalyst poisoning, to remove the smell associated with sulfur and to limit environmental pollutants.

Commercially, these feedstocks can be treated with H₂ over a cobalt promoted molybdenum catalyst supported on Al₂O₃ at temperatures around 400° C.⁶ A mixture of carbon fragments is produced along with H₂S. There are, however, many different forms of organosulfur contaminants present in the feedstocks:⁷ alkyl sulfides, mercaptans and thiophenes are just a few. Thiophenes, being the most resistant to desulfurization, are the focus of most research groups. During HDS, it is believed that thiophene binds to an open Mo site, where a four electron reduction process leads to formation of the observed products.



Despite the importance of HDS, there is still debate over the mechanistic pathways involved. One useful method for understanding the mechanisms of heterogeneous catalysis is to study reactions of related homogeneous systems. Researchers primarily study how thiophenes bind to metal surfaces⁸ or study the reactivity of the organometallic compounds with thiophenes.⁹ Any information obtained may then be extended to the commercial HDS mechanisms.

Thiophene may bind to a metal many different ways (Figure 1.1). The sulfur atom may act as a two electron donor and form an S-M bond, the pi-system may act as a two or four electron donor through one or both olefins or the thiophene may act as a six electron donor through the entire ring system. Depending on the metal and conditions used, any or all binding modes may be seen.¹ Molybdenum and nickel catalysts are used commercially due to their low cost, but other metals such as iridium and rhodium are better HDS catalysts.¹⁰ The activity of a particular catalyst has been related¹⁵ to the percentage of d character of the metal-sulfur bond. That is, greater available d electron density on the metal leads to higher activity. All compounds synthesized for this thesis have iridium centers. See experimental section for details concerning syntheses.

Despite the tremendous importance of HDS, little is certain about the mechanisms involved. Many proposals have been submitted¹¹ but debate still continues. The main discussions involve the initial mode by which the thiophene interacts with the catalyst and whether or not hydrogenation of the C₁-C₂ olefin occurs prior to C-S bond cleavage.

Deuterium exchange studies indicate that the protons alpha to the S atom exchange much faster with M-D than the beta protons. This may be explained¹⁴ by the closer proximity of the alpha protons to the metal surface, given a S-bound thiophene complex. Lipsch and Schuit¹² proposed a "one-point" mechanism in 1969 which involves a S-bound thiophene-metal complex, with no hydrogenation of either double bond, and direct extrusion

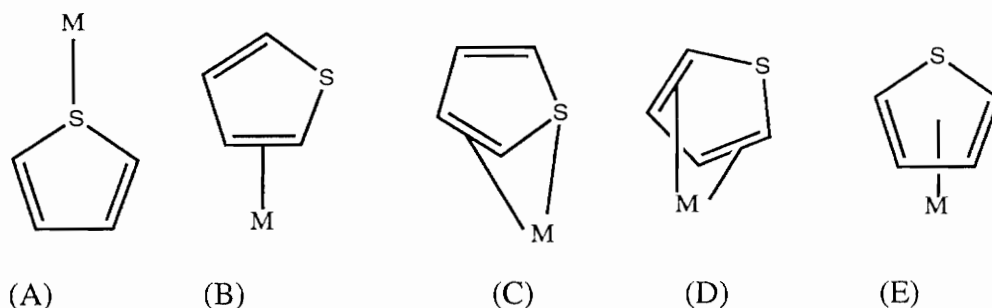


Figure 1.1 Binding modes of thiophene to metals: (A) eta 1 or S- bound, (B) eta 2, (C) eta 3, (D) eta 4 and (E) eta 5.

of a butadiene molecule in one concerted step. (See Figure 1.2) One problem with the one-point mechanism is that it fails to account for the low basicity of the sulfur atom due to charge distribution through the ring.^{8e}

Kwart^{8c} proposed a multi-point mechanism to avoid the low basicity problem associated with the S-bound thiophene molecule. (Figure 1.3) The C₁-C₂ olefin of thiophene binds at a vacancy on the Mo surface allowing the thiophene sulfur to interact with a surface bound sulfur group forming an S-S bond. Binding of the olefin to the metal surface draws electrons away from the sulfur allowing it to bind to an electron rich sulfur on the metal surface. Reduction of the coordinated olefin via addition of protons in a concerted fashion, leads to the dihydrothiophene complex. An elimination reaction leads to formation of final products. This model is also consistent with observed deuterium exchange data. However, an unfavored exo migration of a hydrogen is required.

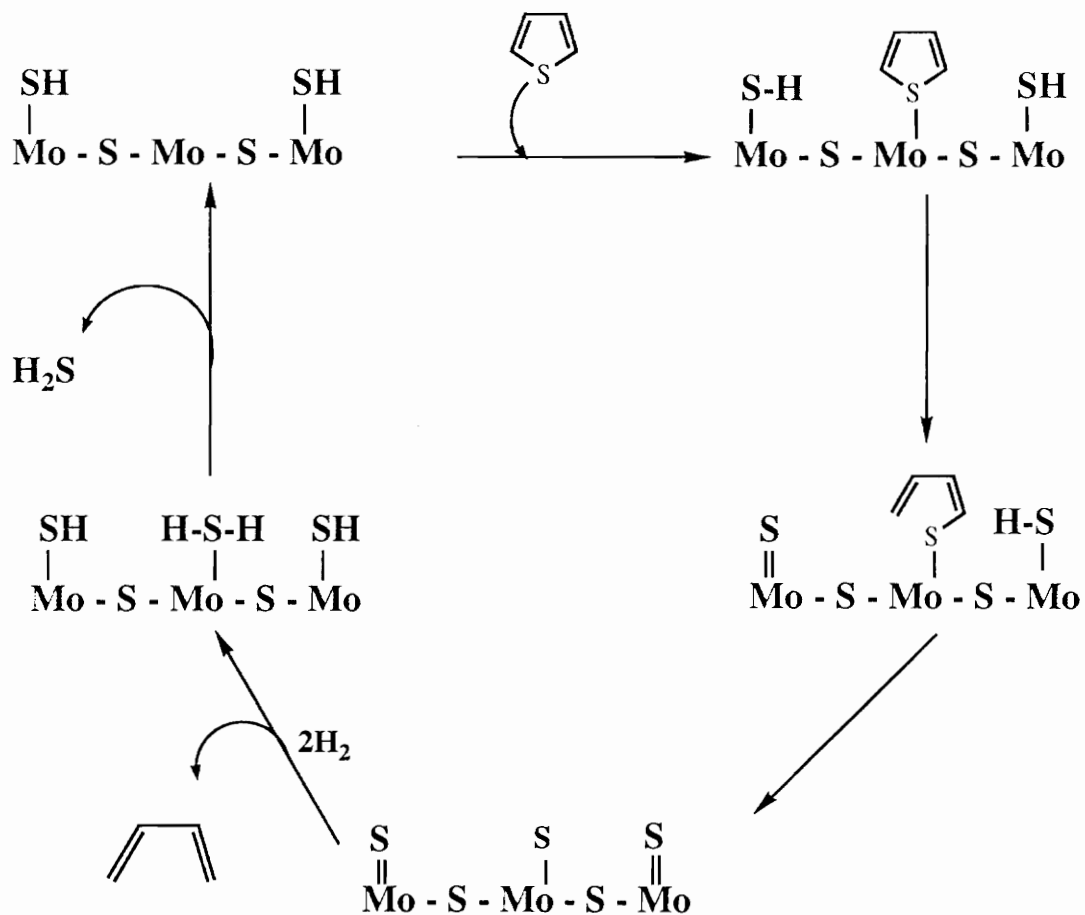


Figure 1.2 The suggested one-point mechanism of thiophene hydrodesulfurization on sulfided Co-Mo/Al₂O₃ and related catalysts.

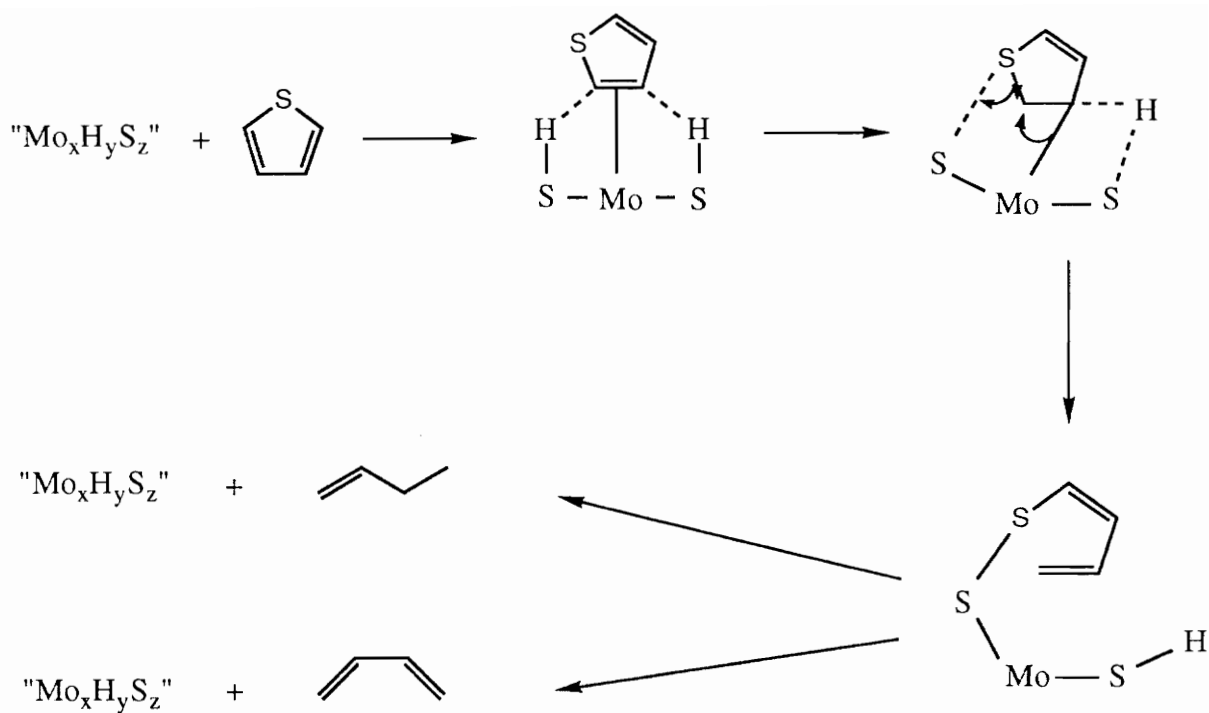
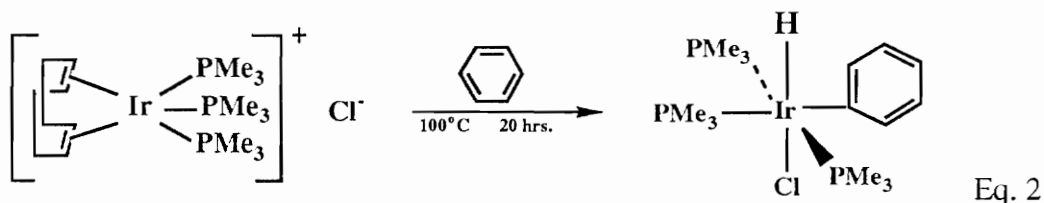


Figure 1.3 The suggested multi-point mechanism of thiophene hydrodesulfurization on sulfided Co-Mo/Al₂O₃ and related catalysts.

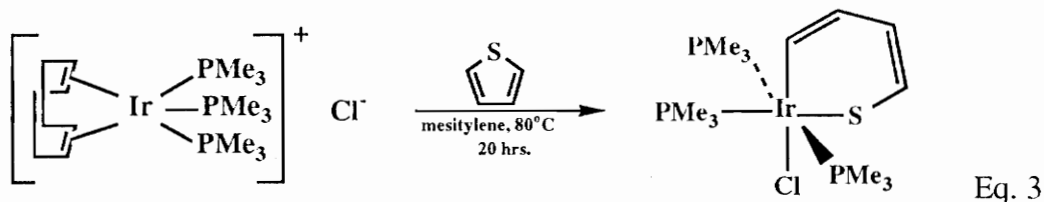
More recent exchange studies¹⁵ with methyl substituted thiophenes indicate that eta-5 coordination may be the cause of the increased deuterium exchange rates for coordinated thiophene. Angelici² proposed a mechanism with an initial eta-5 coordination of thiophene to the metal surface. Hydrogenation of one olefin, via metal hydride and sulfhydryl groups, precedes cleavage of the C-S bond. (See Figure 1.4)

One can conceive another type of mechanism with a metal inserting into the C-S bond of thiophene with or without any further hydrogenation of the ring. In this mechanism the M-S bond would be formed and cleavage of one of the C-S bonds could occur in one step. The first examples of homogeneous ring opened complexes of thiophene were presented by Angelici.² These compounds were formed following oxidative addition of the C-S bond of the thiophene to the Ir metal center. (Figure 1.5) Other examples³ soon followed.

Work of Selnau involved oxidative addition of aromatic compounds to $[\text{Ir}(\text{COD})(\text{PMe}_3)_3]\text{Cl}$. This starting material is formally an Ir(I) species possessing 5 neutral ligands with a chloride ion in the outer sphere. Oxidative addition to the iridium center generates a stable Ir(III) complex. It was shown that benzene reacts (Eq.2) with $[\text{Ir}(\text{COD})(\text{PMe}_3)_3]\text{Cl}$ forming a carbon-iridium sigma bond with the generation of the monohydride complex, $\text{Ir}(\text{Ph})(\text{H})(\text{PMe}_3)_3\text{Cl}$.



Similar complexes are formed when furan and pyridine are used in place of benzene. When this reaction is performed with thiophene (Eq. 3), a different type of complex is formed. The iridium center inserts in the sulfur-carbon bond forming an iridathiabenzene. There are few explanations for this difference in reactivity.



The resonance stabilization energy of furan is poorer than that of thiophene. (The opposite of what one might think given the results.) Could this reactivity then just be an exception or possibly a result of simple thermodynamics. If the iridathiabenzene complex is lower in energy than the possible hydride complex, it might form preferentially. This could be a result of a more stable Ir-S bond, which would in turn lower the overall energy of the complex. The increased electronegativity of oxygen over sulfur may also distort the electronic requirements necessary for formation of the ring-opened complexes. These questions need to be addressed further.

The next logical step would be to investigate the reactivity of $[\text{Ir}(\text{COD})(\text{PMe}_3)_3]\text{Cl}$ with other heteroaromatic compounds to develop a better understanding of this chemistry.

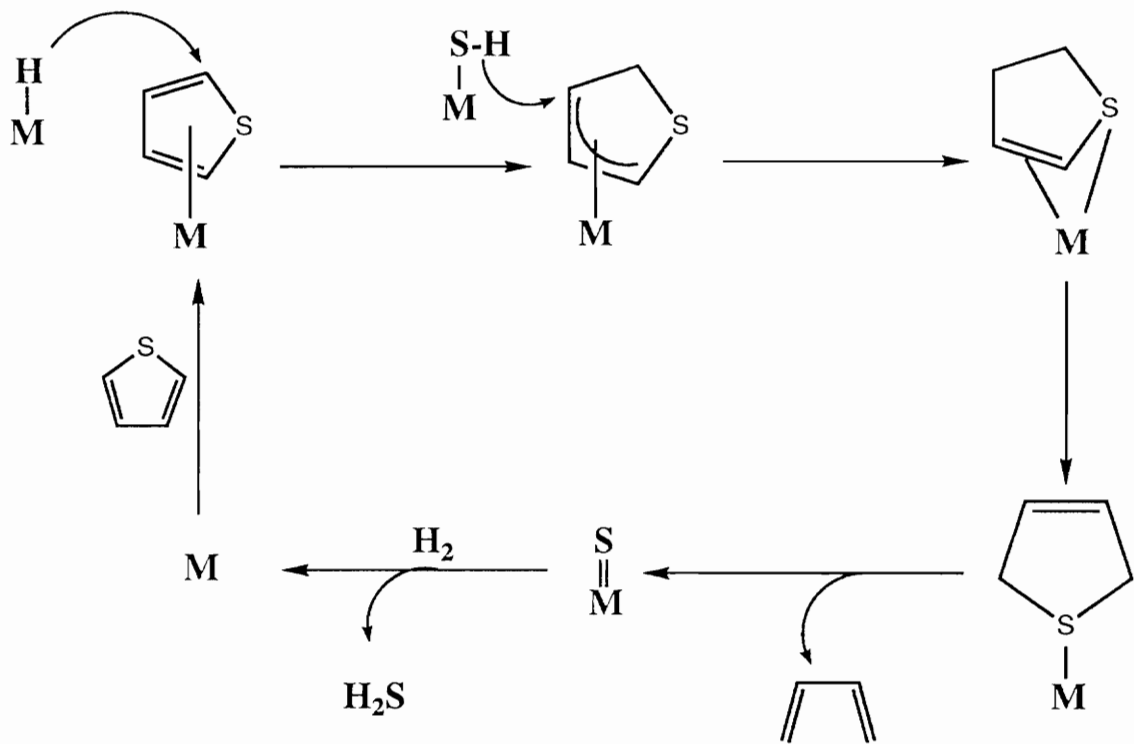


Figure 1.4 A proposed mechanism involving hydrogenation of an olefin prior to C-S cleavage.

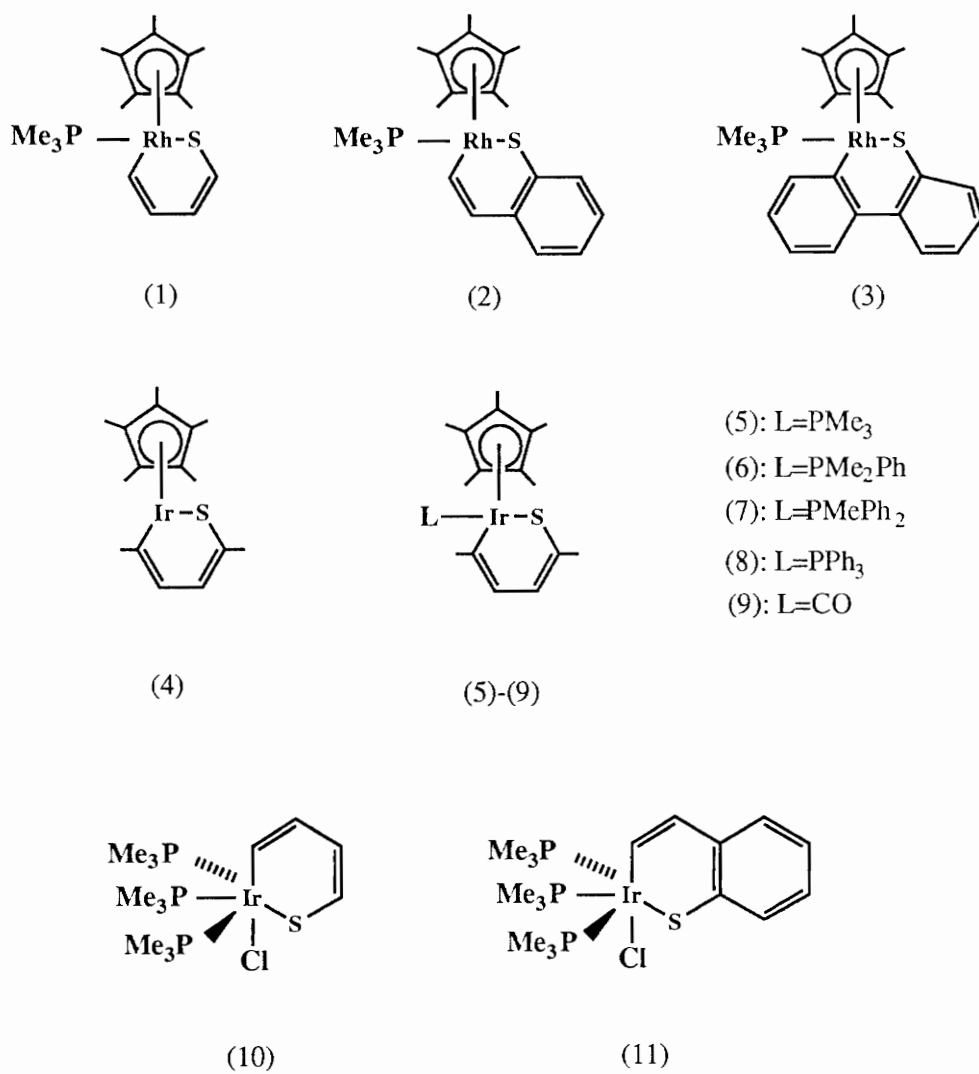


Figure 1.5 Metallacycles formed from C-S insertion of metal complexes: 1&2², 3-9³, 10&11⁴.

Chapter 2: Discussion

Extending the unique reactivity of $[\text{Ir}(\text{COD})(\text{PMe}_3)_3]\text{Cl}$ with thiophene, studies were initiated using other heteroaromatic compounds (Table 2). Significant results were obtained when selenophene as well as certain thiazoles were added to the iridium center. (Figure 2.1)

Table 2. List of heteroaromatic compounds tested for oxidative addition to $[\text{Ir}(\text{COD})(\text{PMe}_3)_3]\text{Cl}$. (Reaction listing of unc. indicates the need for further studies before determining if addition occurs)

<u>Compound</u>	<u>Reaction</u>	<u>Compound</u>	<u>Reaction</u>
selenophene	yes	pyridazine	no
thiazole	yes	oxazole	unc.
4-methylthiazole	yes	isoxazole	unc.
5-methylthiazole	yes	pyrazole	no
benzothiazole	unc.	2,1,3-benzothiadiazole	no

Selenophene was shown to add (Eq. 4) to $[\text{Ir}(\text{COD})(\text{PMe}_3)_3]\text{Cl}$ in the same manner as thiophene. Crystals were grown and x-ray crystallography determined the structure was octahedral with a meridional arrangement of phosphines as was the case with the iridathiabenzene complex.

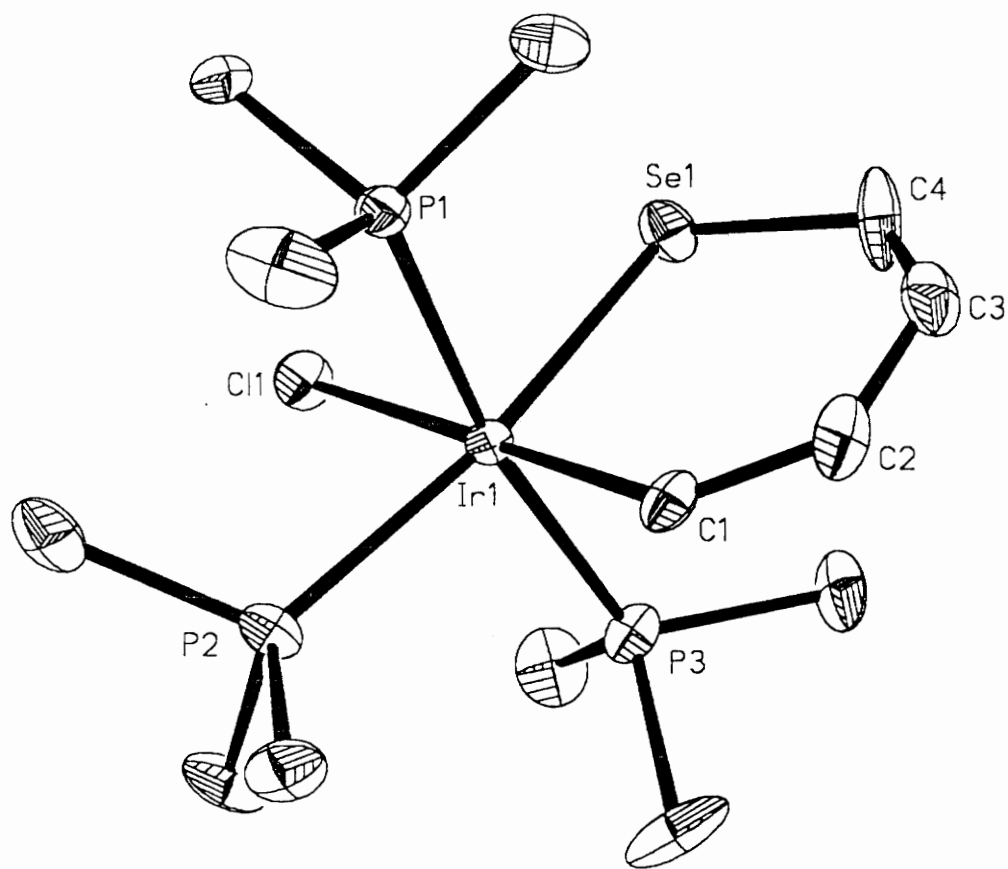
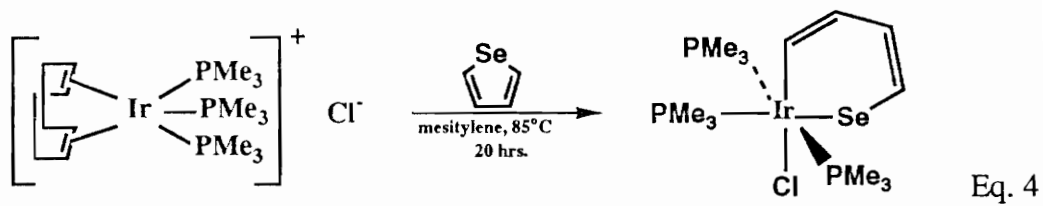


Figure 2.1 ORTEP of $\text{mer}-(\text{Me}_3\text{P})_3\text{Ir}-(\text{CH}=\text{CHCH}=\text{CHSe})\text{Cl}$.

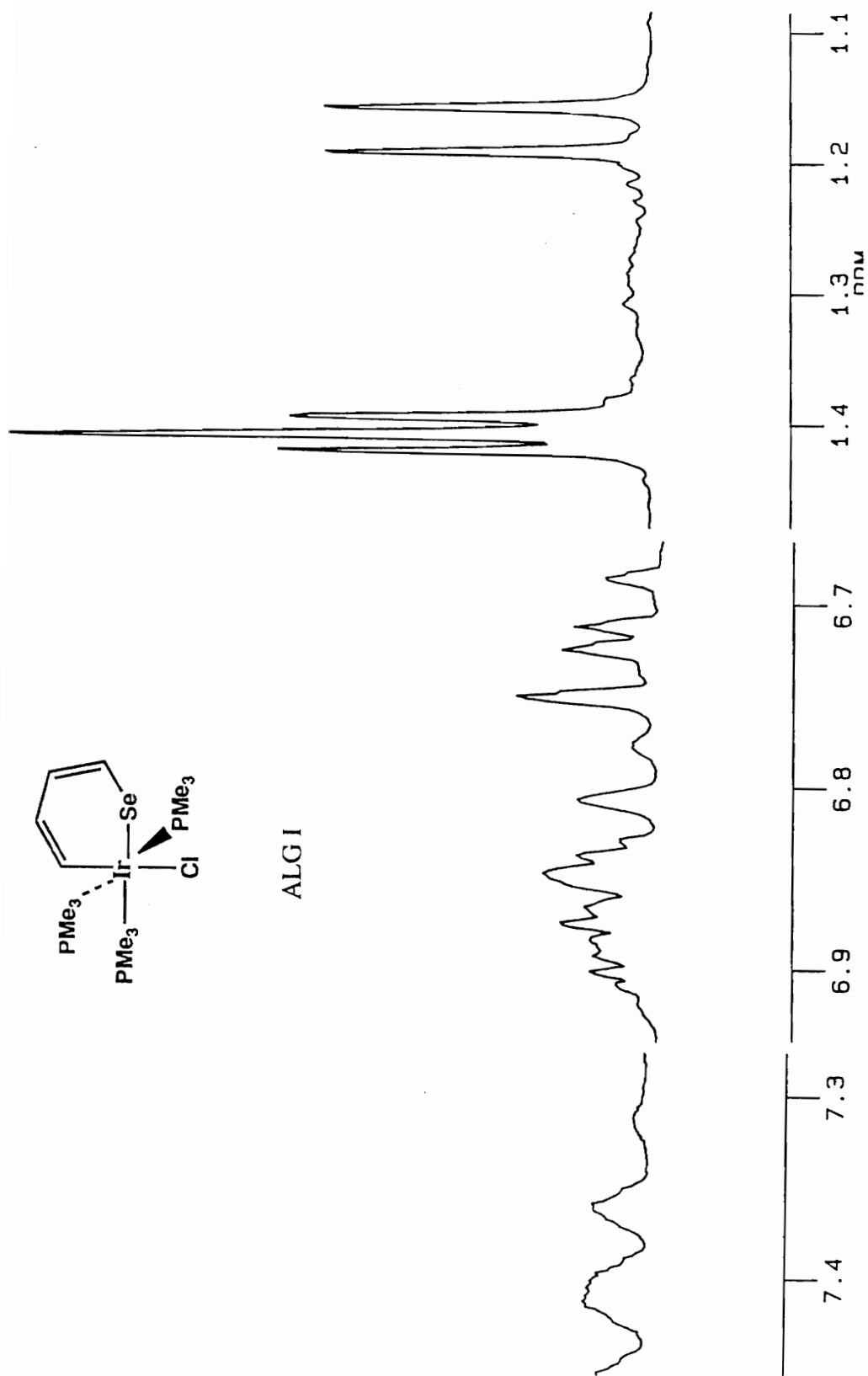


Figure 2.2 ^1H NMR of $\text{mer}-(\text{Me}_3\text{P})_3\text{Ir}-(\text{CH}=\text{CHCH}=\text{CHSe})\text{Cl}$.

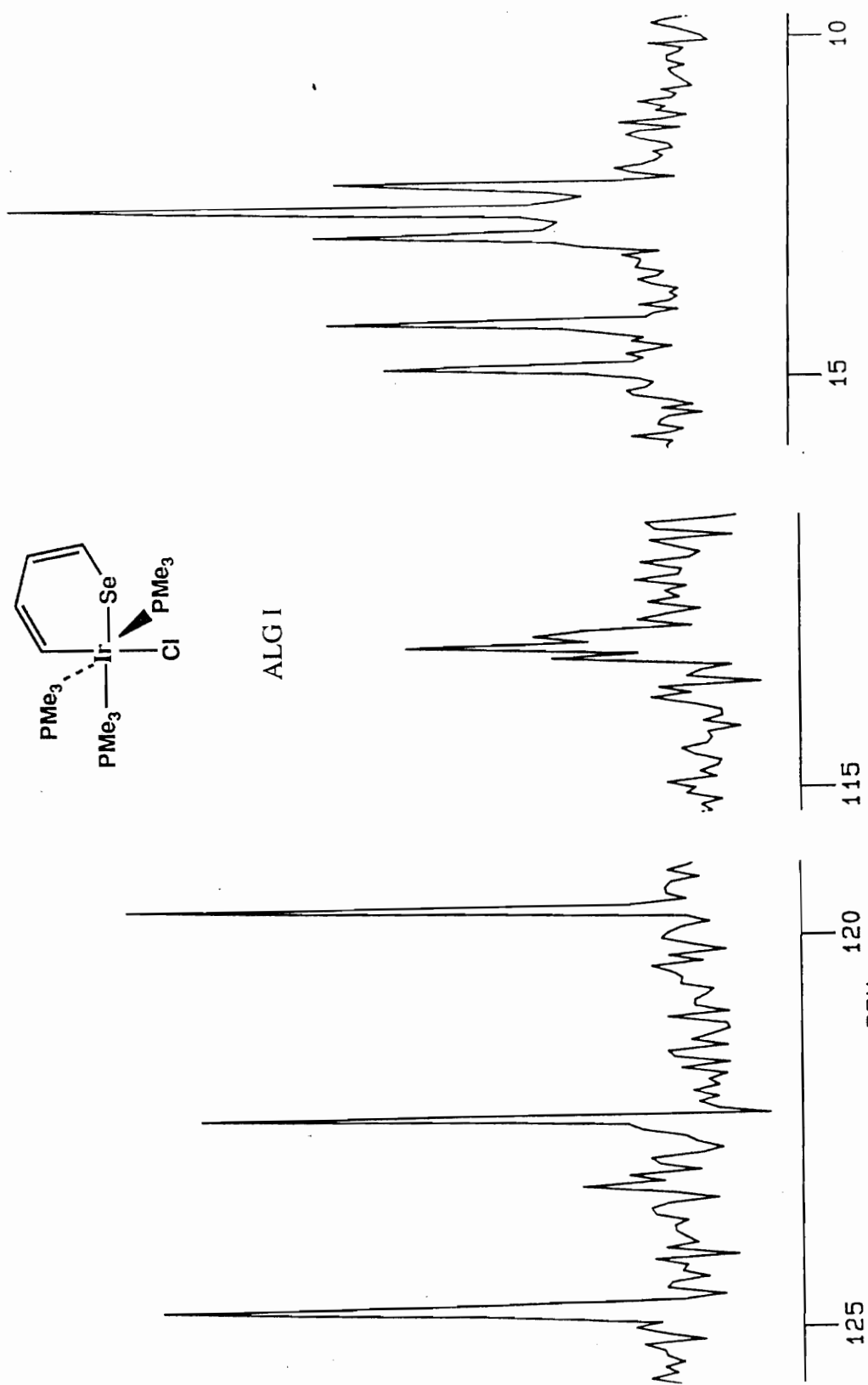


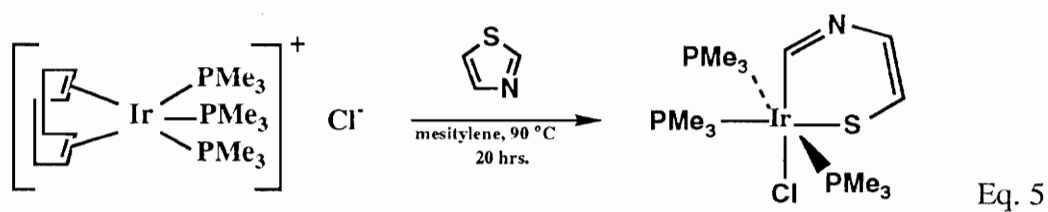
Figure 2.3 ^{13}C NMR of $\text{mer}-(\text{Me}_3\text{P})_3\text{Ir}-(\text{CH}=\text{CHCH}=\text{CHSe})\text{Cl}$.

^1H NMR shows an identifiable set of resonances for the iridium-selenophene complex (a doublet and triplet in the 1-2 ppm range). These resonances, which are also seen for the Ir-thiazole complexes, are due to phosphorous splitting of the hydrogen atoms present on the meridional tertiary phosphines from each molecule. A meridional arrangement of phosphines yields a 2:1 ratio of a triplet and a doublet. A facial arrangement would show three equivalent doublets. This arrangement of phosphines is not seen in any of the reported compounds.

There is also a complex resonance pattern in the aromatic region which corresponds to the protons on the selenophene ring. Integration indicates there are four protons in that region as would be expected.

The Ir-selenophene complex was the first step beyond the iridathiabenzene complex reported by Selnau. In his research, he obtained the crystal structure of the benzothiophene complex. The structure of the Ir-thiophene complex was not reported. The Ir-selenophene complex helps corroborate the proposed structure of the iridathiabenzene complex. Although hydrodeselenation research is not a wide spread as hydrodesulfurization or denitration, the Ir-selenophene might be extended to help study HDSe mechanisms.

Thiazole also adds (Eq. 5) to $[\text{Ir}(\text{COD})(\text{PMe}_3)_3]\text{Cl}$ in the same manner as thiophene and selenophene.



Due to the extra heteroatom in thiazole (compared to thiophene) addition could lead to different isomers (Figure 2.4). Insertion between the carbon-nitrogen bond is possible as well as insertion into the carbon-sulfur bond, although the latter is the only product seen.

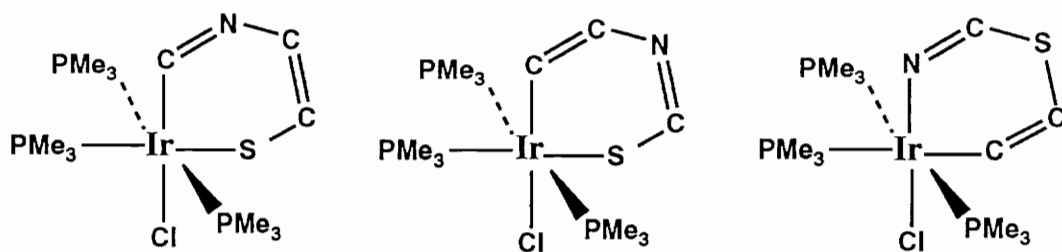


Figure 2.4 Structures of possible isomers of ALG II.

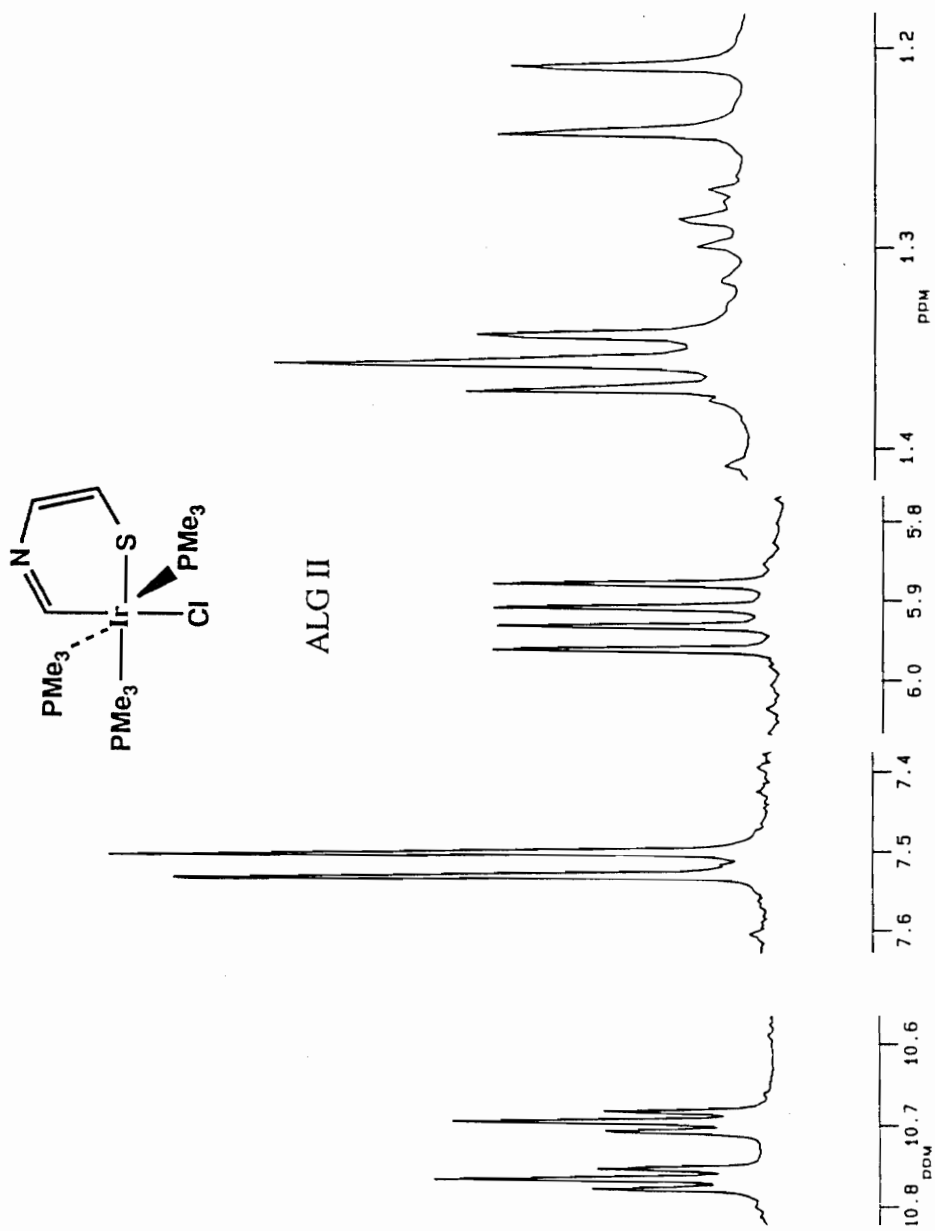


Figure 2.5 ^1H NMR of $\text{mer}-(\text{Me}_3\text{P})_3\text{Ir}(\text{Cl})(\text{CH}=\text{NCH}=\text{CHS})\text{Cl}$.

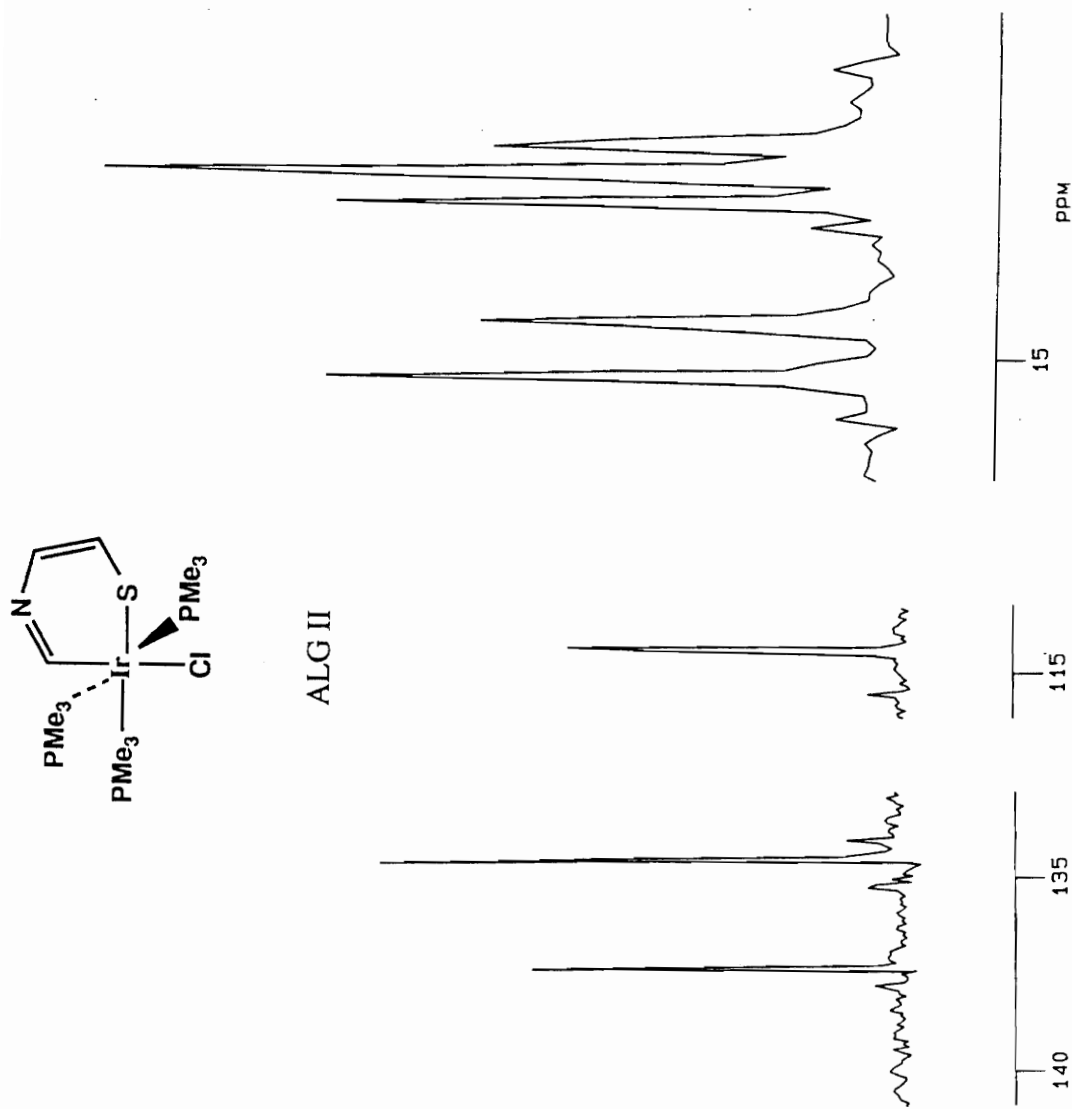
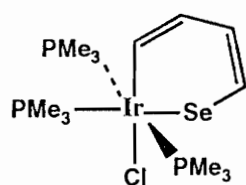
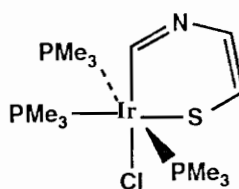


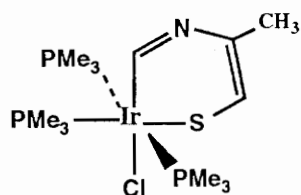
Figure 2.6 ^{13}C NMR of $\text{mer}-(\text{Me}_3\text{P})_3\text{Ir}-(\text{CH}=\text{NCH}=\text{CHS})\text{Cl}$.



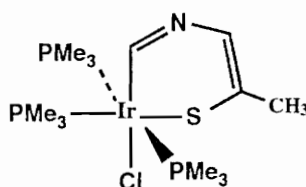
ALG I



ALG II



ALG III



ALG IV

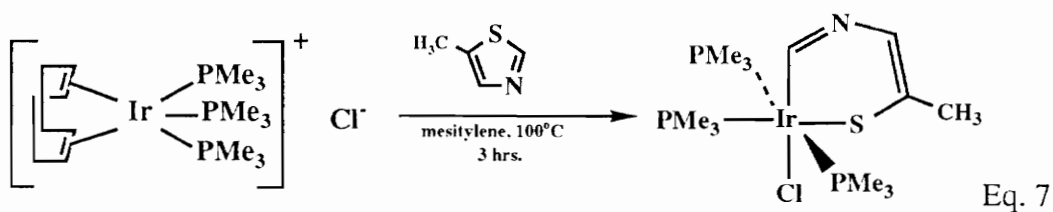
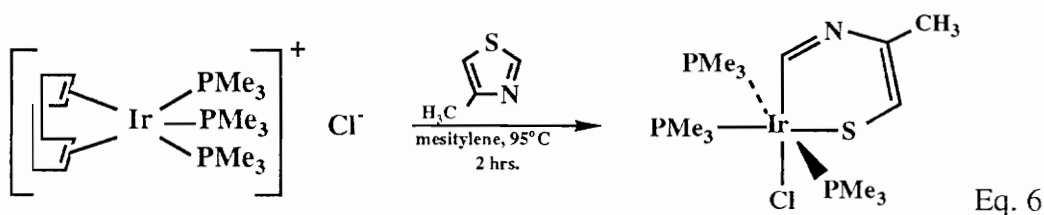
Figure 2.7 Structures of new heteroaromatic metallacycles.

Table 3. ^1H NMR data for Iridium complexes of thiazoles.

<u>Compound</u>	<u>Resonance (^1H NMR)</u>
$(\text{Me}_3\text{P})_3\text{Ir}-(\text{CH}=\text{NCH}=\text{CHS})\text{Cl}$ (ALG II)	1.15, d; 1.36, t; 5.95, dd; 7.56, d 10.77, dt
$(\text{Me}_3\text{P})_3\text{Ir}-(\text{CH}=\text{NC}(\text{CH}_3)=\text{CHS})\text{Cl}$ (ALG III)	1.10, d; 1.32, t; 2.36, s; 5.67, d 10.63, dt
$(\text{Me}_3\text{P})_3\text{Ir}-(\text{CH}=\text{NCH}=\text{C}(\text{CH}_3)\text{S})\text{Cl}$ (ALG IV)	1.16, d; 1.31, t; 2.26, s; 5.62, s 10.40, dt

An interesting anomaly concerning these compounds is the doublet of triplets found far down field (10.4-10.8 ppm) representing the hydrogen atom on the carbon bonded directly to the iridium center for each of the three complexes. These resonances are not from an acid or aldehyde but are well down field of the aromatic region. Any electronic shielding provided by the iridium center should move the resonance up field instead of down field as is thought to occur here.

The other two protons on the thiazole ring of ALG II are seen as a doublet (7.56 ppm) and a doublet of doublets (5.95 ppm). Splitting of the doublet into another doublet occurs due to phosphorous splitting which communicates through the Ir-S-C bond network. The NMR of ALG III, which uses 4-methylthiazole (Eq. 6) in place of neat thiazole, exhibits a doublet (5.67 ppm) only in this region. The presence of this doublet corroborates the phosphorous splitting concept since there is no longer an adjacent proton form the doublet. When 5-methylthiazole is used (Eq. 7) a singlet (5.62 ppm) is seen which is consistent since no splitting by the phosphines should be seen.



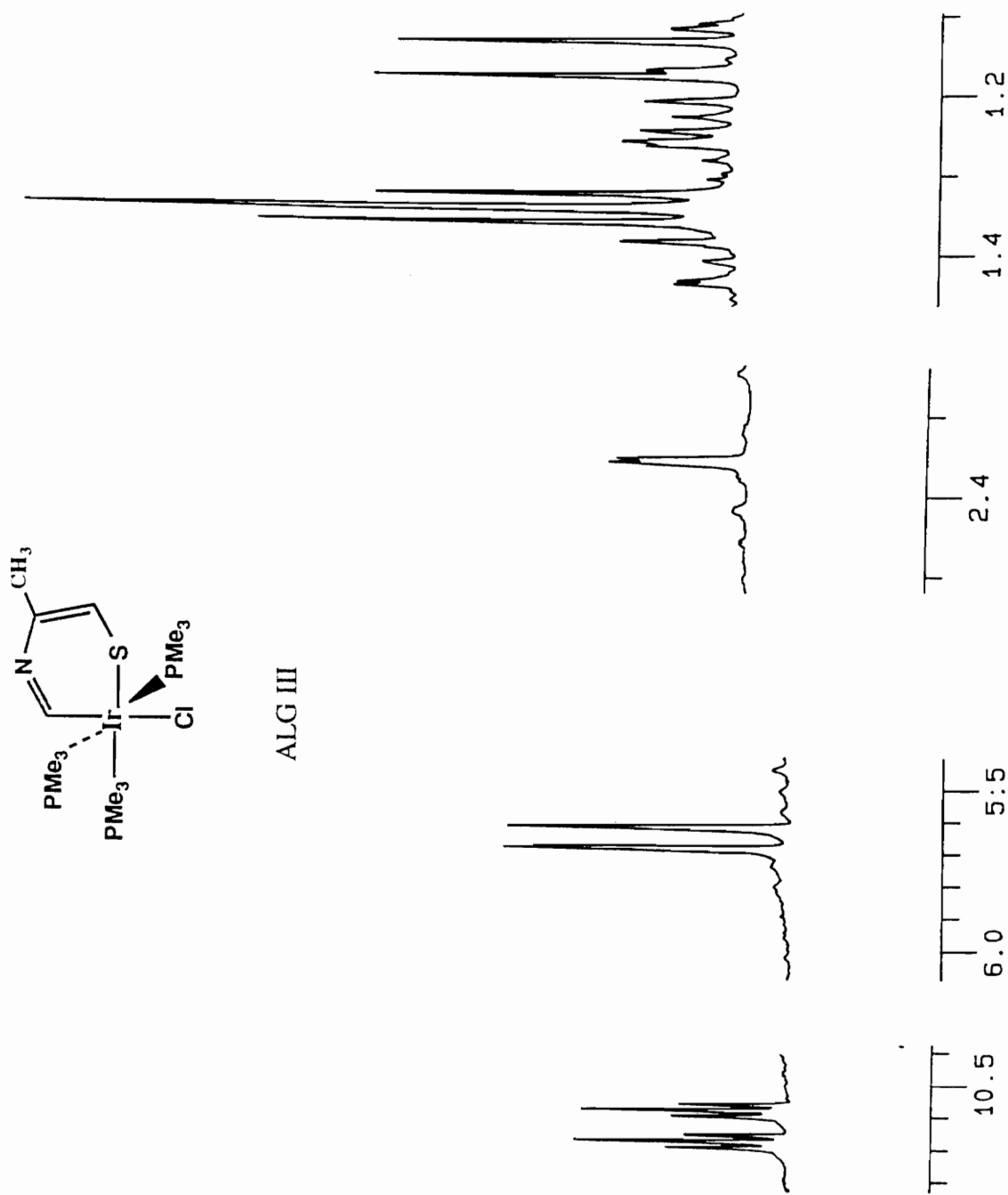
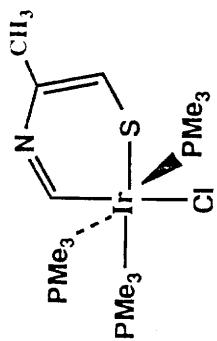


Figure 2.8 ^1H NMR of $\text{mer}-(\text{Me}_3\text{P})_3\text{Ir}-(\text{CH}=\text{NC}(\text{CH}_3)=\text{CHS})\text{Cl}$.



ALG III

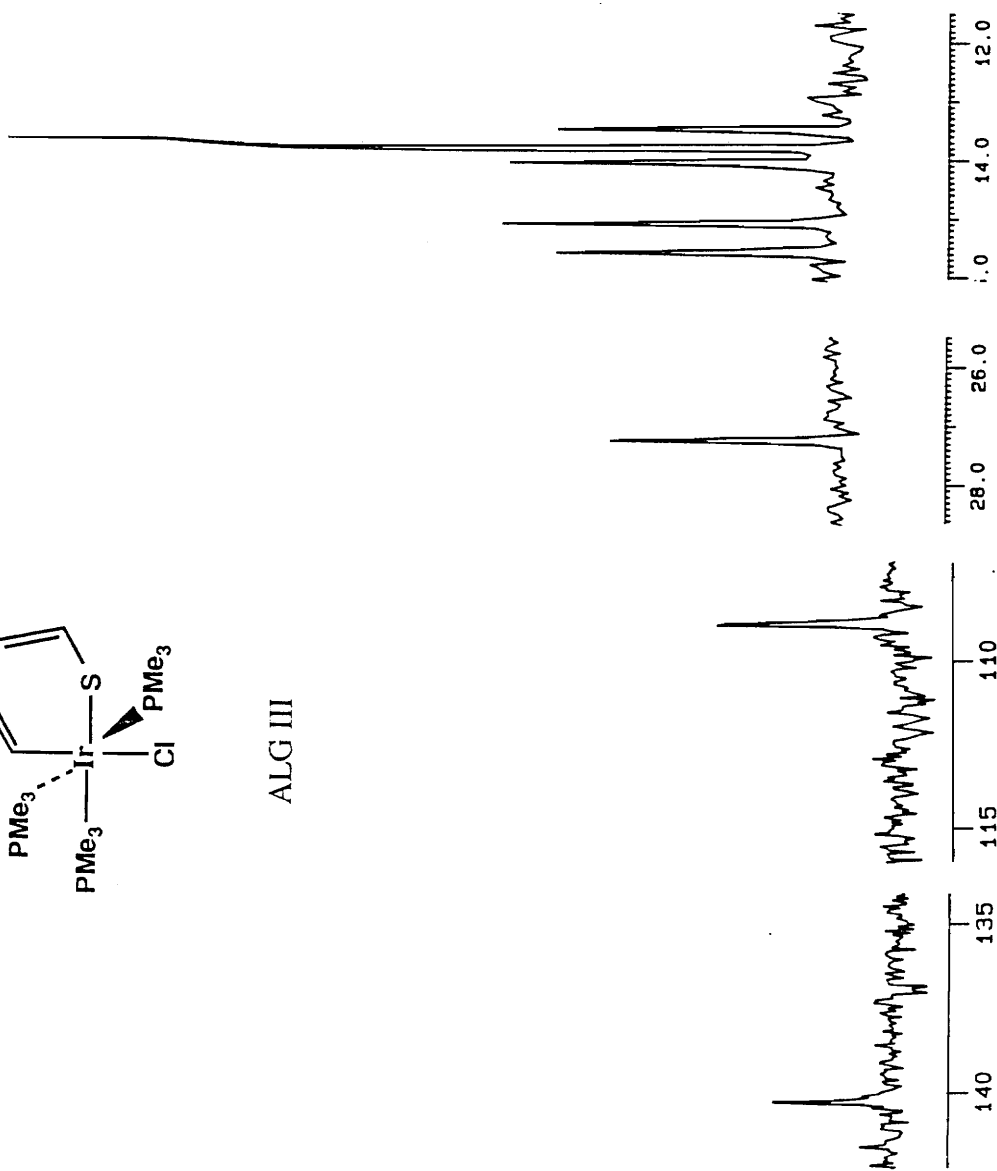
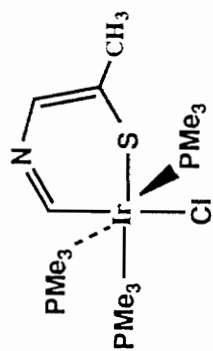


Figure 2.9 ^{13}C NMR of $\text{mer}-(\text{Me}_3\text{P})_3\text{Ir}-(\text{CH}=\text{NC}(\text{CH}_3)=\text{CHS})\text{Cl}$.



ALG IV

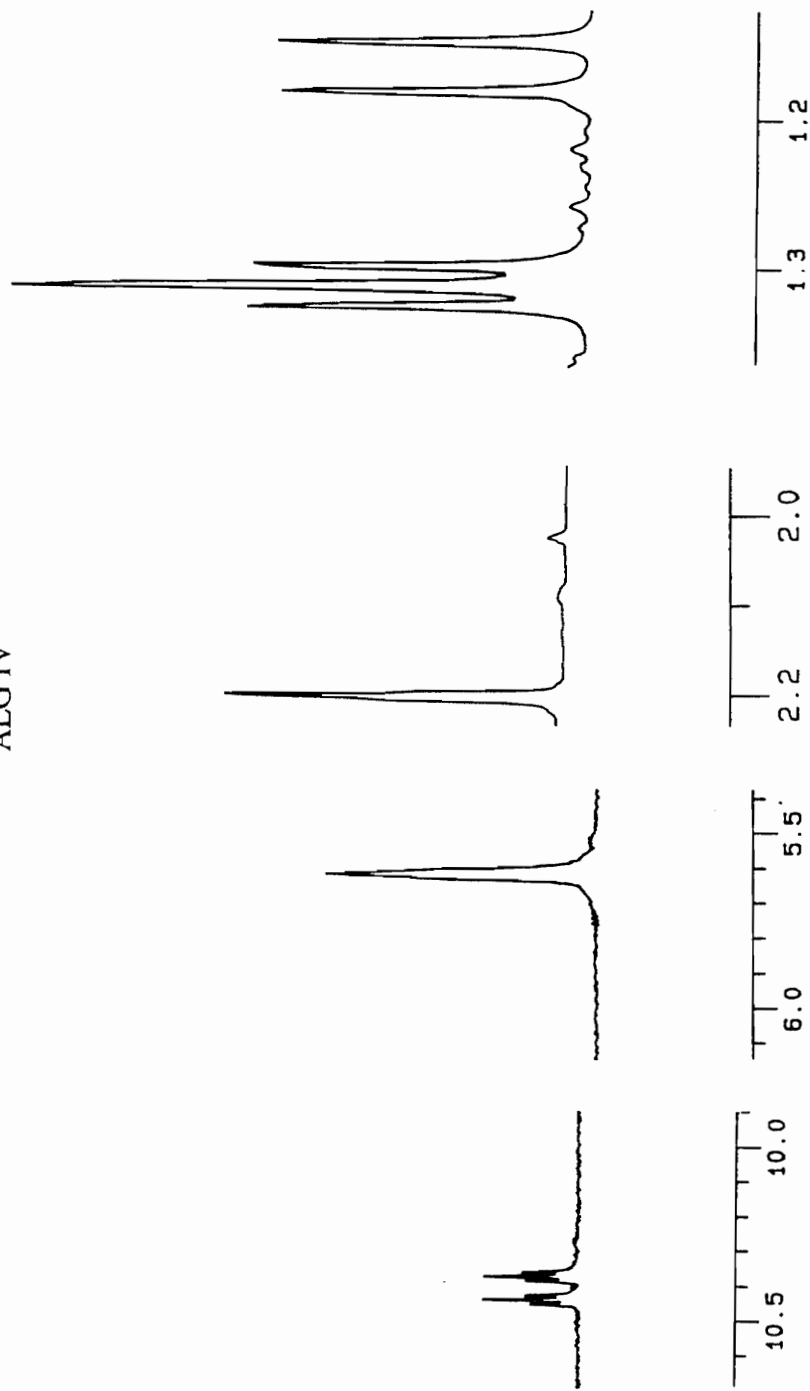
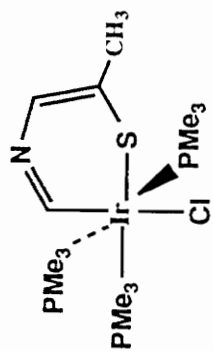


Figure 2.10 ¹H NMR of mer-(Me₃P)₃Ir-(CH=NCH=C(CH₃)₂)S)Cl.



ALG IV

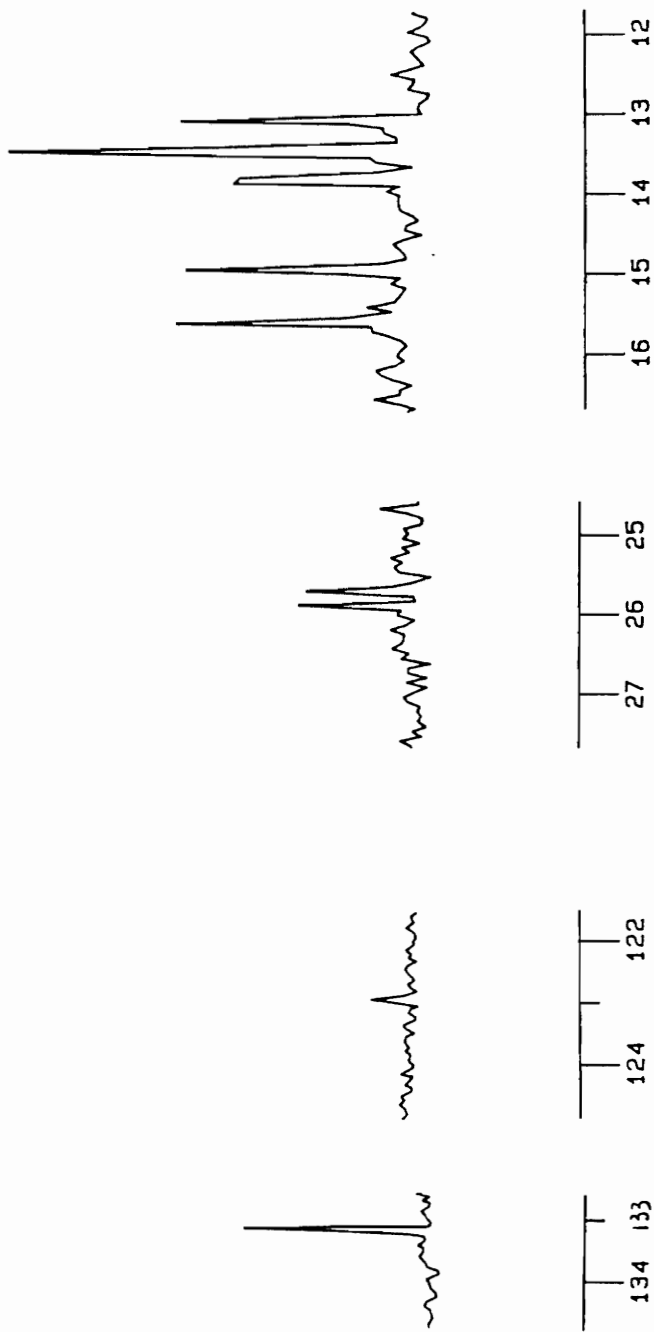


Figure 2.11 ^{13}C NMR of $\text{mer}-(\text{Me}_3\text{P})_3\text{Ir}-(\text{CH}=\text{NCH}=\text{C}(\text{CH}_3)\text{S})\text{Cl}$.

Comparing the ^1H NMR (10.8, 7.4 and 7.2ppm) and ^{13}C NMR (135, 128 and 120 ppm) of ALG II, benzene and the iridathiabenzene compound reported by Selnau, it can be seen that all three compounds are similar in aromaticity.

The compounds described in this thesis are all soluble in water. (100 mg ALG II was found to be soluble in 0.50 mL deionized water.) This is an unusual property for complexes of this type and may be of value for future research.

Following inspection of X-ray crystallography data from the following compounds (Figure 2.12, Tables 4 and 5) it can be seen that all three compounds exhibit similar bond lengths and angles. Substitution of C3 with N distorts these values some, as would be expected, but the values still compare nicely. The length of a C-C bond for benzene is 1.39 Å and the C-C-C angle is 120° . The bond length and angle values for the above compounds are more evidence for the possible aromaticity of the Ir-thiazole complexes.

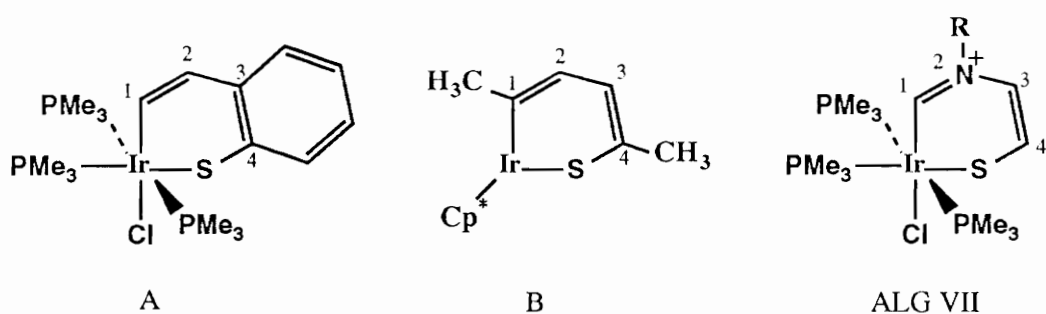


Figure 2.12 Structures of related compounds for comparison. (Dimer ALG VII is used in this comparison in place of ALG II)

Table 4. *Bond Lengths [\AA]:

	A (ref. 4)	B (ref. 9b)	ALG VII
Ir - C1	2.009 (7)	1.986 (6)	1.959 (10)
C1 - C2	1.323 (10)	1.394 (9)	1.321 (15)
C2 - C3	1.461 (11)	1.41 (1)	1.446 (18)
C3 - C4	1.404 (11)	1.375 (9)	1.344 (18)
C4 - S	1.763 (7)	1.713 (6)	1.703 (13)
S - Ir	2.374 (2)	2.203 (2)	2.369 (4)

Table 5. *Bond Angles (degrees):

S-Ir-C1	93.3 (2)	94.3 (2)	84.9 (1)
Ir-C1-C2	131.2 (6)	127.4 (5)	131.3 (9)
C1-C2-C3	131.3 (7)	130.2 (6)	126.8 (9)
C2-C3-C4	126.3 (6)	128.2 (6)	128.4 (12)
C3-C4-S	126.0 (5)	122.6 (5)	130.5 (13)
C4-S-Ir	111.8 (3)	117.2 (2)	106.9 (5)

* For ALG VII: N is substituted for C at the 2 position on the ring.

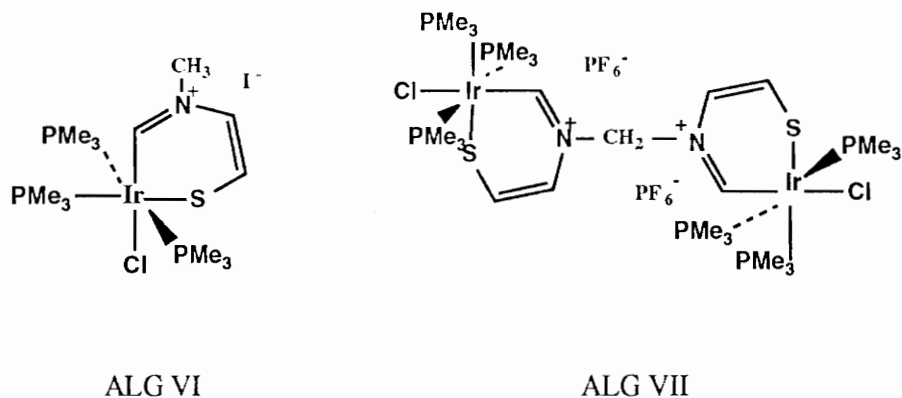


Figure 3.2 Structures of nitrogen substituted complexes.

This phenomenon is thought to be a result of the increased basicity of the complexed thiazole ring which correlates to an increase in nucleophilicity of the complex. The pK_b for uncomplexed thiazole is 11.56 at 20°C¹⁷. This value decreases to approximately 4.8 for the complexed thiazole compound (Fig 3.3). This increase in basicity is evident in the reaction of this complex with halogenated solvents like methylene chloride.

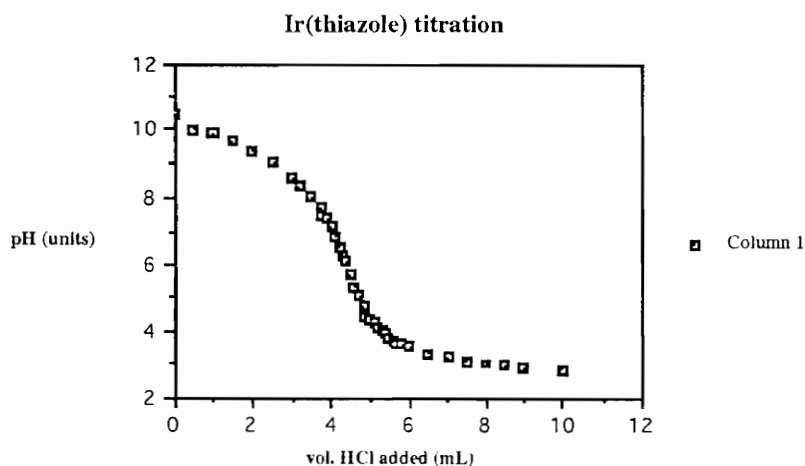


Figure 3.3 Titration curve for ALG II. (90 mg. in 50 mL H₂O, titrated with 0.0121N HCl)

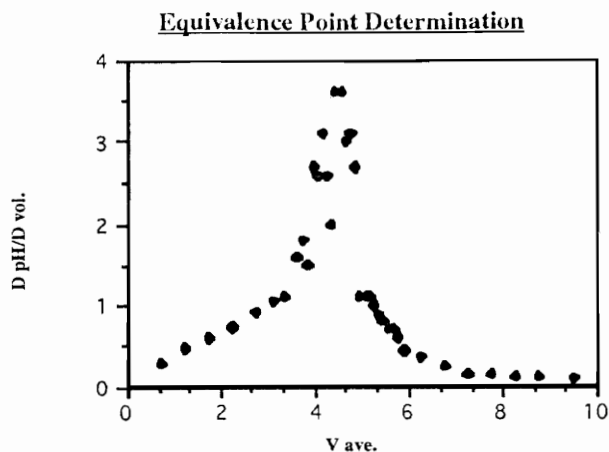


Figure 3.4 Graph for determination of titration equivalence point. A plot of the change in pH divided by the change in volume versus the average volume. (The average volume at the apex is the equivalence point)

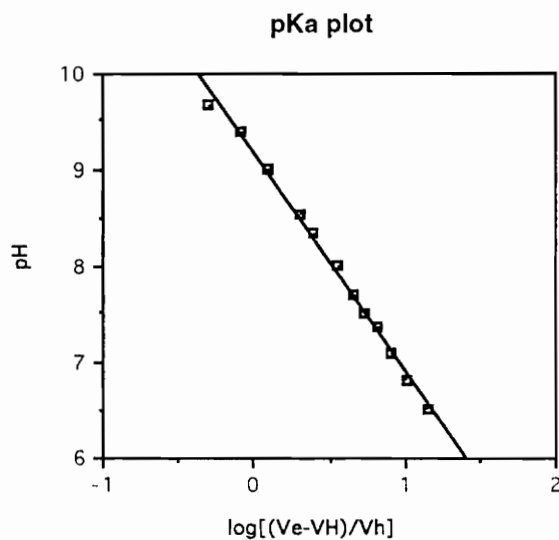


Figure 3.5 Graph for determination of pKa of ALG II. (The slope of the line equals pKa)

The decrease in pK_b may be a result of the disruption of the aromatic character of the complex following insertion of the metal center. Following insertion, the electronic character of the nitrogen lone pair remains localized on the nitrogen. If electronic communication with the rest of the thiazole ring were possible, as with uncomplexed thiazole, the basicity would decrease and the complex would remain stable in halogenated solvents.

When ALG II is dissolved in water a completely different 1H NMR spectra is seen. The doublet of triplets usually found around 10.8 ppm has disappeared, as has the other characteristic resonances of this compound. A doublet of doublets has appeared around 13.7 ppm. A doublet is seen around 8.7 ppm and the proton arrangement between 1-2 ppm which used to indicate a meridional arrangement might suggest change to a facial arrangement. When ALG II is dissolved in methylene chloride a bridged species ALG VII is thought to form. Inspection of the 1H NMR data indicates the presence of a doublet of triplets around 11.7 ppm as well as the doublet and doublet of doublets seen from ALG II. For the bridged species the doublet of doublets is found further downfield (7.0 ppm) than the doublet (6.5 ppm) reversed from what is seen from ALG II. This NMR data is not conclusive, however, and further research is necessary.

Chapter 4: Conclusion

The impetus for this research lies in the previously mentioned work by Selnau. Studies of C-H activation with aromatic compounds lead to the discovery of a ring-opened thiophene complex. Extending this work to heteroaromatic compounds, many possible models have been synthesized which may help shed light on the elusive hydrodesulfurization and hydrodenitration mechanisms.

Selenophene, thiazole and two substituted thiazoles all form interesting complexes when reacted with the iridium starting material. The work with selenophene was a simple extension of the work performed by Selnau and served to corroborate his thiophene research and proved a good connection to the thiazole research presented.

Further areas of research must include thorough studies of iridium centers with other heteroaromatic compounds (quinoline, isoquinoline, triazine, pyrazine...). These studies should also include heteroaromatic compounds with electron withdrawing and donating substituents to best understand the addition mechanisms.

Following a move to reduce the use of toxic solvents, aqueous chemistry research has gained popularity. The complexes reported in this thesis are soluble in water which, although unusual for compounds similar to these, may prove to be a useful property for future research. Attempted syntheses in D₂O have failed, but considerable research still remains unexplored.

The reactivity of complexes reported here should also be investigated for possible reactions with acetylenes, olefins or any other reactive, unsaturated compounds. Synthesis of rhodium analogs may prove more revealing since iridium complexes are generally less reactive than rhodium complexes. This should allow for a more in depth look at the reactivity of these complexes.

Although this thesis poses more questions than it answers, a rich new area of research has been opened, which offers genuine research opportunities for many to follow.

Chapter 5: Experimental Section

General Comments

An inert atmosphere was maintained during all reaction manipulations. This was accomplished with a double barrel manifold (Schlenk line). House nitrogen was the source of inert gas. Dry box manipulations were performed in a MB-150-M glove box purchased from M. Braun, Germany. Iridium chloride ($\text{IrCl}_3 \cdot 3\text{H}_2\text{O}$) was purchased from Johnson Matthey and used without further purification. All solvents used were purchased from Fischer Scientific or Aldrich Chemical Company and were dried by standard methods. All reactants were purchased from Aldrich Chemical Company and were used without further purification. NMR spectra were obtained with Bruker model WP-200 and WP-270 NMR spectrometers. X-ray crystal structures were determined with a Siemens model R3m/v diffractometer and SHELXTL-PLUS software. Samples were shipped to Atlantic Microlab Incorporated.

^1H NMR: benzene- d_6 , $\delta=7.15$

^{13}C NMR: benzene- d_6 , $\delta=128.0$ ppm

^{31}P NMR: H_3PO_4 (an internal reference, inside a sealed ampule), $\delta=0.0$ ppm

Experimental Section

Synthesis of $[\text{Ir}(\text{COD})(\text{PMe}_3)_3]\text{Cl}$: Starting Material

Reference #16

Synthesis of $\text{mer}-(\text{Me}_3\text{P})_3\text{Ir}-(\text{CH}=\text{CHCHCH}=\text{S})\text{Cl}$

Reference #4

Synthesis of $\text{mer}-(\text{Me}_3\text{P})_3\text{Ir}-(\text{CH}=\text{CHCHCH}=\text{Se})\text{Cl}$ (ALG I)

In a dry box, $[\text{Ir}(\text{COD})(\text{PMe}_3)_3]\text{Cl}$ (0.50 g, 0.89 mmol) was placed inside a Teflon screw-capped reaction tube and sealed with a septum. The reaction tube was then removed to a hood where dry mesitylene (7.0 mL) and selenophene (0.25 mL, 2.71 mmol) were added under nitrogen. The reaction tube was sealed with a Teflon screw-cap, placed in an oil bath (85^o C), stirred for 24 hours and cooled to room temperature. During that time the solution color changed from white to orange. The orange solution was filtered into a side-arm flask with a filter cannula and product precipitated out of solution by the addition of dry pentane (50 mL). Recovered crystals were washed with dry pentane (2 x 25 mL) and dried under vacuum.

Experimental yield was 0.391 g. (75% based on $[\text{Ir}(\text{COD})(\text{PMe}_3)_3]\text{Cl}$). ¹H NMR (C₆D₆): δ 1.18 (d, $J_{\text{P-H}}=9.12$ Hz, 9H, PMe_3), 1.40 (t, $J_{\text{P-H}}=3.50$ Hz, 18 H, PMe_3), 6.80 (m, 2H) and 7.42 ppm (m, 2H). ¹³C NMR (C₆D₆): δ 12.58 (t, $J_{\text{P-C}}=81.1$ Hz, trans PMe_3), 14.66 (d, $J_{\text{P-C}}=138.0$ Hz, cis PMe_3), 111.27 (q, $J_{\text{P-C}}=36.6$ Hz) and 119.48, 125.94 and 126.59 ppm (s, selenophene) ³¹P NMR (C₆D₆): δ -50.35 (t, $J=20.10$ Hz, trans PMe_3) and -43.44 ppm (d, $J=20.79$ Hz, cis PMe_3) Elemental analysis observed for ALG I: C=27.17%; H=5.40% (Calculated values: 26.608 and 5.325)

Synthesis of mer-(Me₃P)₃Ir-(CH=NCH=CHS)Cl**(ALG II)**

In a dry box, [Ir(COD)(PMe₃)₃]Cl (0.50 g, 0.89 mmol) was placed inside a Teflon screw-capped reaction tube and sealed with a septum. The reaction tube was then removed to a hood where dry mesitylene (6.0 mL) and thiazole (0.40 mL, 5.64 mmol) were syringed in under nitrogen. The reaction tube was sealed with a Teflon screw-cap, placed in an oil bath (85^o C), stirred for 24 hours and cooled to room temperature. During that time the solution color changed from white to orange. The orange solution was filtered into a side-arm flask with a filter cannula and product precipitated out of solution by the addition of dry pentane (50 mL). Recovered crystals are washed with dry pentane (2 x 25 mL) and dried under vacuum.

Experimental yield was 0.399 g. (83% based on [Ir(COD)(PMe₃)₃]Cl). ¹H NMR (C₆D₆): δ 1.21 (d, J_{P-H}=8.91 Hz, 9H, cis PMe₃), δ 1.36 (t, J_{P-H}=3.78 Hz, 18H, trans PMe₃), δ 5.92 (dd, J_{H-H}= 6.52, J_{P-H}=21.74, 1H), δ 7.51 (d, J_{H-H}=8.70 Hz, 1H) and δ 10.73 ppm (dt, J_{P-H}=19.1 Hz, J_{H-H}=3.91 Hz, 1H) ¹³C NMR (C₆D₆): δ 13.33 (t, J_{P-C}=76.94 Hz, trans PMe₃), δ 14.56 (d, J_{P-C}=132.90 Hz, cis PMe₃), δ 114.8 (s, thiazole), δ 126.5 (s, thiazole) and δ 134.0 ppm (s, thiazole). ³¹P NMR (CD₃CN): δ -43.73 (t, J=20.15 Hz, trans PMe₃) and δ -40.00 ppm (d J=20.38 Hz, cis PMe₃). Elemental analysis observed for ALG II: C=26.47%; H=5.63% (Calculated values: 26.640 and 5.589)

Synthesis of mer-(Me₃P)₃Ir-(CH=NC(CH₃)=CHS)Cl**(ALG III)**

In a dry box, [Ir(COD)(PMe₃)₃]Cl (0.50 g, 0.89 mmol) was placed inside a Teflon screw-capped reaction tube and sealed with a septum. The reaction tube was then removed to a hood where dry mesitylene (6.0 mL) and 4-methyl thiazole (0.45 mL, 4.95 mmol) were syringed in under nitrogen. The reaction tube was sealed with a Teflon screw-cap, placed in an oil bath (95^o C), stirred for 3 hours and cooled to room temperature. During that time the solution color changed from white to orange. The orange solution was filtered into a side-arm flask with a filter cannula and product precipitated out of solution by the addition of dry pentane (50 mL). Recovered crystals are washed with dry pentane (2 x 25 mL) and dried under vacuum.

Experimental yield was 0.421 g. (86% based on [Ir(COD)(PMe₃)₃]Cl). ¹H NMR (C₆D₆): δ 1.10 (d, J_{P-H}=8.70 Hz, 9H, cis PMe₃), δ 1.32 (t, J_{P-H}=3.48 Hz, 18H, trans PMe₃), δ 2.36 (d, J_{H-H}=1Hz, 3H), δ 5.66 (d, J_{H-H}=13.04 Hz, 1H), and δ 10.63 ppm (dt, J_{P-H}=19.1, J_{H-H}=3.76 Hz, 1H) ¹³C NMR (C₆D₆): δ 13.69 (t, J_{P-C}=20.86 Hz, trans PMe₃), δ 15.20 (d, J_{P-C}=33.40 Hz, cis PMe₃), δ 22.59 (s, methyl), δ 108.87 (s, thiazole), δ 126.85 (s, thiazole) and δ 140.25 ppm (s, thiazole). ³¹P NMR (C₆D₆): δ -42.26 (d, J=20.52 Hz, trans PMe₃) and δ -43.90 ppm (t, J=20.90 Hz, cis PMe₃) Elemental analysis observed for ALG III: C=27.88%; H=5.79% (Calculated values: 28.131 and 5.811)

Synthesis of mer-(Me₃P)₃Ir-(CH=NCH=C(CH₃)S)Cl**(ALG IV)**

In a dry box, [Ir(COD)(PMe₃)₃]Cl (0.50 g, 0.89 mmol) was placed inside a Teflon screw-capped reaction tube and sealed with a septum. The reaction tube was then removed to a hood where dry mesitylene (6.0 mL) and 5-methyl thiazole (0.30 mL, 3.39 mmol) were syringed in under nitrogen. The reaction tube was sealed with a Teflon screw-cap, placed in an oil bath (95^o C), stirred for 48 hours and cooled to room temperature. During that time the solution color changed from white to orange. The orange solution was filtered into a side-arm flask with a filter cannula and product precipitated out of solution by the addition of dry pentane (50 mL). Recovered crystals are washed with dry pentane (2 x 25 mL) and dried under vacuum.

Experimental yield was 0.361 g. (73% based on [Ir(COD)(PMe₃)₃]Cl). ¹H NMR (C₆D₆): δ 1.10 (d, J_{P-H}=8.79 Hz, 9H, cis PMe₃), δ 1.32 (t, J_{P-H}=3.77 Hz, 18H, trans PMe₃), δ 2.22 (s, 3H), δ 5.62 (s, 1H) and δ 10.40 ppm (dt, J_{P-H}=18.04 Hz J_{H-H}=3.43 Hz, 1H) ¹³C NMR (C₆D₆): δ 13.50 (t, J_{P-C}=19.73 Hz, trans PMe₃), δ 15.25 (d, J_{P-C}=34.53 Hz, cis PMe₃), δ 28.40 (s, methyl), δ 123 ppm (s, thiazole), δ 127.15 (s, thiazole) and δ 132.10 ppm (s, thiazole). ³¹P NMR (C₆D₆): δ - 41.15 (t, J= 21.09 Hz, trans PMe₃) and δ -42.30 ppm (t, J= 20.89 Hz, cis PMe₃) Elemental analysis observed for ALG IV: C=29.98%; H=5.95% (Calculated values: 28.131 and 5.811)

Synthesis of mer-(Me₃P)₃Ir-(CH=N(CH₃)CH=CHS)I

(ALG VI)

(Me₃P)₃Ir-(CH=NCH=CHS)Cl (25.0 mg, 4.60 x 10⁻² mmol) was placed inside a NMR reaction tube and sealed with a septum. The reaction tube was removed to a hood where d₆-benzene (0.5 mL) and iodomethane (6.0 μL, 9.65 x 10⁻² mmol) were syringed in under nitrogen. The reaction tube was allowed to stand at room temperature for 20 hours. NMR data was obtained from the solution which appeared to be converted to mostly the single product (ALG VI).

¹H NMR (C₆D₆): δ 1.13 (d, J_{P-H}=8.95 Hz, 9H, cis PMe₃), δ 1.34 (t, J_{P-H}=3.85 Hz, 18H, trans PMe₃), δ 3.02 (s, 3H), δ 5.97 (dd, J_{H-H}= 6.88, J_{P-H}=22.07; 1H); δ 5.66 (d, J_{H-H}=8.05 Hz, 1H) and δ 10.40 ppm (dt, J_{P-H}=18.15 Hz J_{H-H}=3.71 Hz, 1H)

References

1. Angelici, R.J. *Accounts of Chemical Research* **1988**, v. 21, 11, 387-94
2. Chen, J.; Daniels, L.M.; Angelici, R.J. *J. Am. Chem. Soc.* **1990**, 112, 199
3. Jones, W.D.; Dong, L. *J. Am. Chem. Soc.* **1991**, 113, 559
4. Selnau, H.E. *Ph.D. Thesis*, VPI & SU, 1992
5. (a) McCulloch, D.C. In *Applied Industrial Catalysis*; Leach, B.E., Ed.; Academic: New York, 1983; Vol. 1, p. 69 (b) Schuman, S.C.; Shalit, H. *Catal. Rev.* 1970, 4, 245
6. Weisser, O.; Landa, S. *Sulfide Catalysts: Their Properties and Applications*; Pergamon: Oxford, 1973
7. Lyapina, N.K.; Kamyranov, V.F. In *Organic Sulfur Chemistry*; Freidina, R. Kh., Skorova, A.E., Eds.; Pergamon: New York, 1981; p. 201
8. (a) Markel, E.J.; Schrader, G.L.; Sauer, N.N.; Angelici, R.J. *J. Catal.* **1989**, 116, 11-22
(b) Stohr, J.; Gland, J.L.; Kollin, E.B.; Muetterties, E.L. *Phys. Rev. Lett.* **1984**, 53, 2161.
(c) Kwart, H.; Schuit, G.C.A.; Gates, B.C. *J. Catal.* **1980**, 61, 128-34 (d) Givens, K.E.; Dillard, J.G. *J. Catal.* **1984**, 86, 108-20 (e) Prins, R.; De Beer, V.H.J.; Somorjai, G.A. *Catal. Rev. - Sci. Eng.* **1989**, 31(1&2), 1-41

9. (a) Chen, J.; Su, Y.; Jacobson, R.; Angelici, R.J. *J. Organomet. Chem.* **1992**, 415-429
(b) Chen, J.; Daniels, L.M.; Angelici, R.J. *J. Am. Chem. Soc.* **1991**, 113, 2544-2552 (c)
Chin, R.M.; Jones, W.D. *Angew. Chem. Int. Ed. Engl.* **1992**, 31(3), 357 (d) Chen, J.;
Angelici, R.J. *Organomet.* **1992**, 11, 992-6 (e) Hockett, S.C.; Angelici, R.J.
Organomet. **1988**, 7, 1491-1500 (f) Chen, J.; Angelici, R.J. *Organomet.* **1990**, 9, 849-
52
10. Harris, S.; Chianelli, R.R. *J. Catal.* **1986**, 98, 17
11. (a) Lesch, D.A.; Richardson, J.W.; Jacobson, R.A.; Angelici, R.J. *J. Am. Chem. Soc.*
1984, 106, 2901 (b) Dong, L.; Duckett, S.B.; Ohman, K.F.; Jones, W.D. *J. Am. Chem.*
Soc. **1992**, 114, 151-60 (d) Hachgenei, J.W.; Angelici, R.J. *J. Organomet. Chem.* **1988**,
355, 359-78
12. Lipsch, J.M.J.G.; Schuit, G.C.A. *J. Catal.* **1969**, 15, 179
13. Smith, G.V., Hinckley, C.C., Behbahany, F. *J. Catal.* **1973**, 30, 218
14. Sauer, N.N., Angelici, R.J. *Organometallics* **1987**, 6, 1146
15. Pecorraro, T.A., Chianelli, R.R. *J. Catal.* **1981**, 67, 430
16. Selnau, H. E.; Merola, J.S. *J. Am. Chem. Soc.* **1991**, 113, 4008
17. Weast, R.C. *CRC Handbook of Chemistry and Physics*, **1986** D-160

Appendix

X-ray Crystallographic Data

STRUCTURE DETERMINATION SUMMARY for mer-(Me₃P)₃Ir(SeCHCHCHCH)(Cl)**Crystal Data**

Empirical Formula C₁₃ H₃₁ Cl Ir P₃ Se
 Color; Habit orange irregular
 Crystal Size (mm) 0.4 x 0.4 x 0.3
 Crystal System Tetragonal
 Space Group P4₃
 Unit Cell Dimensions a = 9.164(2) Å
 c = 24.427(8) Å

Volume 2051.2(11) Å³

Z 4

Formula Weight 586.9

Density(calc.) 1.900 Mg/m³

Absorption Coefficient 8.636 mm⁻¹

F(000) 1128

Data Collection

Diffractionmeter Used Siemens R3m/V
 Radiation MoK_α (λ = 0.71073 Å)

Temperature (K) 298

Monochromator Highly oriented graphite crystal

2θ Range 3.5 to 55.0°

Scan Type Wyckoff

Scan Speed Variable; 3.97 to 19.53°/min. in w

Scan Range (ω) 0.60°

Background Measurement Stationary crystal and stationary counter at beginning and end of scan, each for 25.0% of total scan time

Standard Reflections 3 measured every 300 reflections

Index Ranges 0 < h < 11, 0 < k < 11, -31 < l < 31

Reflections Collected 5301

Independent Reflections 4700 (R_{int} = 5.34%)

Observed Reflections 3595 (F > 4.0σ(F))

Absorption Correction Semi-empirical

Min./Max. Transmission 0.5578 / 0.9820

Solution and Refinement

System Used Siemens SHELXTL PLUS (VMS)

Solution Direct Methods

Refinement Method Full-Matrix Least-Squares

Quantity Minimized Σw(F_o-F_c)²

Absolute Structure h = -1.02(4)

Extinction Correction c = 0.00027(5), where

F* = F [1 + 0.002cF²/sin(2θ)]^{-1/4}

Riding model, fixed isotropic U

w⁻¹ = s²(F) + 0.0017F²

Number of Parameters Refined 173

Final R Indices (obs. data) R = 5.55 %, wR = 6.73 %

Goodness-of-Fit 1.10

Largest and Mean D/s 0.029, 0.005

Data-to-Parameter Ratio 20.8:1

Largest Difference Peak 3.62 eÅ⁻³

Table 1. Atomic coordinates ($\times 10^4$) and equivalent isotropic displacement coefficients ($\text{\AA}^2 \times 10^3$) for mer-(Me₃P)₃Ir{SeCHCHCHCH}(Cl)

	x	y	z	U (eq)
Ir (1)	644 (1)	4182 (1)	1149	30 (1)
P (1)	2101 (6)	5691 (6)	605 (2)	49 (2)
P (2)	2517 (5)	2617 (6)	1373 (2)	46 (2)
P (3)	-1003 (5)	3070 (5)	1760 (2)	42 (2)
Cl (1)	183 (6)	2432 (6)	398 (2)	55 (2)
Se (1)	-1536 (2)	5481 (2)	762 (1)	54 (1)
C (1)	1022 (20)	5657 (18)	1765 (7)	42 (6)
C (2)	340 (26)	6900 (21)	1878 (7)	59 (8)
C (3)	-948 (26)	7530 (23)	1642 (9)	62 (8)
C (4)	-1716 (32)	7160 (20)	1227 (10)	81 (10)
C (11)	1455 (29)	7506 (21)	483 (10)	81 (10)
C (12)	3782 (29)	6266 (34)	901 (11)	106 (13)
C (13)	2518 (32)	5084 (31)	-78 (10)	89 (11)
C (21)	3579 (22)	2980 (26)	1977 (9)	63 (7)
C (22)	3913 (22)	2332 (28)	844 (9)	74 (9)
C (23)	1979 (25)	718 (25)	1454 (9)	72 (9)
C (31)	-242 (28)	2457 (34)	2414 (10)	95 (12)
C (32)	-2420 (23)	4193 (26)	2036 (10)	69 (8)
C (33)	-2014 (20)	1557 (21)	1485 (10)	63 (8)

* Equivalent isotropic U defined as one third of the trace of the orthogonalized U_{ij} tensor

Table 2. Bond lengths (Å) for

Ir(1)-P(1)	2.338 (5)	P(2)-C(22)	1.836 (21)
Ir(1)-P(2)	2.303 (5)	P(2)-C(23)	1.820 (24)
Ir(1)-P(3)	2.354 (5)	P(3)-C(31)	1.832 (25)
Ir(1)-Cl(1)	2.473 (5)	P(3)-C(32)	1.789 (23)
Ir(1)-Se(1)	2.510 (2)	P(3)-C(33)	1.798 (21)
Ir(1)-C(1)	2.053 (16)	Se(1)-C(4)	1.920 (21)
P(1)-C(11)	1.790 (21)	C(1)-C(2)	1.328 (26)
P(1)-C(12)	1.782 (27)	C(2)-C(3)	1.435 (32)
P(1)-C(13)	1.799 (25)	C(3)-C(4)	1.279 (34)
P(2)-C(21)	1.798 (21)		

mer-(Me₃P)₃Ir{SeCHCHCHCH}(Cl)
Table 3. Bond angles (°) for

P(1)-Ir(1)-P(2)	94.4(2)	C(12)-P(1)-C(13)	106.5(13)
P(1)-Ir(1)-P(3)	169.4(2)	Ir(1)-P(2)-C(21)	118.9(8)
P(2)-Ir(1)-P(3)	93.3(2)	Ir(1)-P(2)-C(22)	116.2(7)
P(1)-Ir(1)-Cl(1)	93.4(2)	C(21)-P(2)-C(22)	103.1(10)
P(2)-Ir(1)-Cl(1)	84.2(2)	Ir(1)-P(2)-C(23)	114.8(7)
P(3)-Ir(1)-Cl(1)	94.6(2)	C(21)-P(2)-C(23)	103.6(11)
P(1)-Ir(1)-Se(1)	87.7(1)	C(22)-P(2)-C(23)	97.4(11)
P(2)-Ir(1)-Se(1)	168.0(1)	Ir(1)-P(3)-C(31)	116.2(8)
P(3)-Ir(1)-Se(1)	86.2(1)	Ir(1)-P(3)-C(32)	117.1(8)
Cl(1)-Ir(1)-Se(1)	83.8(1)	C(31)-P(3)-C(32)	97.1(12)
P(1)-Ir(1)-C(1)	86.1(5)	Ir(1)-P(3)-C(33)	115.3(8)
P(2)-Ir(1)-C(1)	96.3(5)	C(31)-P(3)-C(33)	106.6(12)
P(3)-Ir(1)-C(1)	85.9(5)	C(32)-P(3)-C(33)	102.2(10)
Cl(1)-Ir(1)-C(1)	179.2(5)	Ir(1)-Se(1)-C(4)	103.0(8)
Se(1)-Ir(1)-C(1)	95.6(5)	Ir(1)-C(1)-C(2)	129.6(14)
Ir(1)-P(1)-C(11)	117.1(9)	C(1)-C(2)-C(3)	130.5(18)
Ir(1)-P(1)-C(12)	115.9(9)	C(2)-C(3)-C(4)	131.6(21)
C(11)-P(1)-C(12)	94.5(13)	Se(1)-C(4)-C(3)	129.3(19)
Ir(1)-P(1)-C(13)	117.8(9)		

mer-(Me₃P)₃Ir{SeCHCHCHCH}(Cl)

C(11)-P(1)-C(13)	101.7(12)
------------------	-----------

Table 4. Anisotropic displacement coefficients ($\text{\AA}^2 \times 10^3$) for mer-(Me₃P)₃Ir{SeCHCHCH}(Cl)

	U ₁₁	U ₂₂	U ₃₃	U ₁₂	U ₁₃	U ₂₃
Ir (1)	32 (1)	34 (1)	25 (1)	-1 (1)	-3 (1)	-1 (1)
P (1)	65 (3)	46 (3)	35 (3)	-14 (2)	5 (2)	-2 (2)
P (2)	41 (2)	61 (3)	38 (2)	11 (2)	-2 (2)	-2 (2)
P (3)	38 (2)	42 (3)	47 (3)	1 (2)	3 (2)	8 (2)
Cl (1)	62 (3)	58 (3)	46 (3)	-2 (2)	-10 (2)	-20 (2)
Se (1)	56 (1)	58 (1)	48 (1)	16 (1)	-14 (1)	2 (1)
C (1)	57 (11)	38 (9)	29 (8)	-16 (8)	10 (8)	0 (7)
C (2)	101 (18)	46 (11)	29 (9)	-6 (11)	4 (10)	-27 (8)
C (3)	80 (16)	53 (13)	54 (13)	12 (11)	20 (12)	-12 (10)
C (4)	162 (24)	30 (9)	51 (14)	31 (12)	-4 (16)	12 (10)
C (11)	118 (21)	40 (12)	83 (17)	10 (12)	58 (16)	27 (11)
C (12)	107 (21)	134 (26)	76 (17)	-88 (20)	-17 (16)	25 (17)
C (13)	118 (23)	100 (20)	49 (13)	9 (17)	23 (15)	7 (13)
C (21)	55 (12)	83 (15)	50 (11)	-13 (11)	-21 (10)	3 (11)
C (22)	49 (12)	117 (20)	54 (13)	32 (12)	0 (10)	-39 (13)
C (23)	71 (15)	85 (17)	61 (14)	26 (12)	-33 (12)	-4 (12)
C (31)	75 (17)	159 (28)	50 (13)	23 (16)	7 (12)	51 (16)
C (32)	57 (13)	82 (16)	68 (14)	2 (11)	37 (11)	-1 (12)
C (33)	34 (10)	55 (12)	102 (18)	-8 (8)	-3 (10)	13 (12)

The anisotropic displacement exponent takes the form: $-2p^2(h^2a^2U_{11} + \dots + 2hka^*b^*U_{12})$

Table 5. H-Atom coordinates ($\times 10^4$) and isotropic displacement coefficients ($\text{\AA}^2 \times 10^3$) for

mer-(Me₃P)₃Ir{SeCHCHCHCH}(Cl)

	x	y	z	U
H(1A)	1823	5415	2002	80
H(2A)	739	7453	2176	80
H(3A)	-1260	8432	1804	80
H(4A)	-2535	7773	1143	80
H(11A)	2130	8032	256	80
H(11B)	529	7440	300	80
H(11C)	1336	8009	824	80
H(12A)	4298	6877	648	80
H(12B)	3599	6799	1233	80
H(12C)	4360	5419	983	80
H(13A)	3119	5787	-262	80
H(13B)	3030	4172	-54	80
H(13C)	1629	4949	-279	80
H(21A)	4317	2243	2014	80
H(21B)	4033	3922	1953	80
H(21C)	2945	2955	2290	80
H(22A)	4633	1658	976	80
H(22B)	3525	1987	503	80
H(22C)	4354	3272	791	80
H(23A)	2821	143	1544	80
H(23B)	1280	658	1746	80
H(23C)	1549	354	1122	80
H(31A)	-1012	2028	2626	80
H(31B)	508	1745	2351	80
H(31C)	160	3273	2609	80
H(32A)	-3028	3641	2280	80
H(32B)	-1981	4988	2232	80
H(32C)	-3001	4570	1741	80
H(33A)	-2649	1179	1763	80
H(33B)	-2586	1891	1180	80
H(33C)	-1362	802	1365	80

STRUCTURE DETERMINATION SUMMARY for [mer-(Me₃P)₃Ir(SCHCHNCH)(Cl)]CH₂**Crystal Data**

Empirical Formula C₂₅ H₆₂ Cl₂ F₁₂ Ir₂ N₂ P₈ S₂
 Color; Habit yellow rectangular plate
 Crystal Size (mm) 0.08 x 0.22 x 0.60
 Crystal System Triclinic
 Space Group P-1
 Unit Cell Dimensions

a = 12.737(6) Å

b = 13.390(6) Å

c = 15.053(8) Å

a = 99.28(4)°

b = 101.35(4)°

g = 101.30(3)°

2415(2) Å³

Volume

Z

2

Formula Weight

1385.9

Density(calc.)

1.906 Mg/m³

Absorption Coefficient

6.037 mm⁻¹

F(000)

1348

Data Collection

Diffractometer Used

Siemens R3m/V

Radiation

MoK_α (λ = 0.71073 Å)

Temperature (K)

298

Monochromator

Highly oriented graphite crystal

2θ Range

3.5 to 45.0°

Scan Type

Wyckoff

Scan Speed

Variable; 3.97 to 14.65°/min. in w

Scan Range (w)

0.60°

Background Measurement

Stationary crystal and stationary counter at beginning and end of scan, each for 25.0% of total scan time

Standard Reflections

3 measured every 300 reflections

Index Ranges

0 < h < 13, -14 < k < 14, -16 < l < 15

Reflections Collected

6565

Independent Reflections

6223 (R_{int} = 2.02%)

Observed Reflections

4864 (F > 3.0s(F))

Solution and Refinement

System Used

Siemens SHELXTL PLUS (VMS)

Solution

Direct Methods

Refinement Method

Full-Matrix Least-Squares

Quantity Minimized

Sw(F_o-F_c)²

Extinction Correction

c = 0.00005(2), where

F* = F [1 + 0.002cF²/sin(2q)]^{-1/4}

Hydrogen Atoms

Riding model, fixed isotropic U

Weighting Scheme

w⁻¹ = s²(F) + 0.0011F²

Number of Parameters Refined

479

Final R Indices (obs. data)

R = 4.65 %, wR = 5.31 %

Goodness-of-Fit

1.10

Largest and Mean D/s

0.297, 0.058

Data-to-Parameter Ratio

10.2:1

Table 1. Atomic coordinates ($\times 10^4$) and equivalent isotropic displacement coefficients ($\text{\AA}^2 \times 10^3$) for mer-(Me₃P)₃Ir{SCHCHNCH}(Cl)

	x	y	z	U(eq)
Ir(1)	4346(1)	7081(1)	8038(1)	33(1)
Cl(1)	5932(3)	8492(3)	8906(3)	57(1)
P(1)	3305(3)	7453(3)	9149(2)	50(1)
P(2)	3883(3)	8356(3)	7235(3)	47(1)
P(3)	5354(3)	6491(3)	6955(3)	49(1)
S(1)	5123(3)	6060(3)	9014(3)	54(1)
C(1)	3068(10)	5967(9)	7349(8)	36(5)
N(1)	2805(8)	4968(7)	7370(6)	34(4)
C(2)	3430(12)	4422(10)	7950(10)	57(6)
C(3)	4352(11)	4816(11)	8626(10)	59(6)
C(11)	3984(14)	8514(13)	10132(10)	81(8)
C(12)	1972(11)	7681(12)	8731(10)	67(7)
C(13)	2916(13)	6399(13)	9726(10)	73(7)
C(21)	3827(13)	9566(11)	7972(11)	71(7)
C(22)	4875(14)	8945(12)	6652(13)	86(9)
C(23)	2619(12)	8022(12)	6383(10)	72(7)
C(31)	6666(12)	7365(12)	7000(12)	75(8)
C(32)	4605(16)	6186(14)	5751(11)	96(10)
C(33)	5769(15)	5289(12)	7048(13)	90(9)
C(101)	1777(9)	4279(9)	6774(8)	39(5)
Ir(2)	-222(1)	2178(1)	8071(1)	36(1)
Cl(1A)	-1413(3)	1317(3)	8956(3)	71(2)
P(1A)	-1851(3)	2446(3)	7164(3)	53(2)
P(2A)	-347(3)	632(3)	7032(3)	63(2)
P(3A)	1245(3)	1924(4)	9184(3)	64(2)
S(1A)	-132(4)	3751(3)	9125(3)	65(2)
C(1A)	776(10)	2908(8)	7397(8)	35(5)
N(1A)	1011(8)	3907(7)	7360(7)	37(4)
C(2A)	614(12)	4736(10)	7796(11)	57(6)
C(3A)	155(11)	4717(10)	8537(10)	55(6)
C(11A)	-2962(13)	1311(14)	6713(15)	108(10)
C(12A)	-2543(14)	3243(15)	7782(12)	92(9)
C(13A)	-1755(14)	3049(14)	6197(11)	83(8)
C(21A)	-1300(14)	-505(11)	7140(15)	103(10)
C(22A)	-743(15)	661(14)	5816(12)	100(9)
C(23A)	911(13)	201(12)	6992(13)	83(8)
C(31A)	2589(11)	2207(13)	8967(12)	80(8)
C(32A)	1443(20)	2629(21)	10316(13)	154(16)
C(33A)	1126(15)	636(16)	9417(16)	122(13)
P(4)	-693(4)	6434(4)	5948(3)	71(2)
F(1)	-1166(11)	6023(13)	6759(8)	147(8)
F(2)	441(9)	6161(10)	6334(9)	129(7)
F(3)	-240(8)	6768(9)	5119(7)	104(6)
F(4)	-1761(12)	6761(15)	5629(11)	187(11)
F(5)	-1173(12)	5332(10)	5345(9)	150(8)
F(6)	-150(16)	7544(11)	6574(12)	212(11)
P(4A)	3591(4)	1790(4)	5935(3)	71(2)
F(1A)	3186(13)	1582(10)	4895(8)	145(8)
F(2A)	3232(16)	595(9)	5924(11)	176(10)
F(3A)	3995(23)	2007(15)	6976(10)	250(16)

F(4A)	3818(14)	2979(9)	5926(11)	176(9)
F(5A)	4696(12)	1729(21)	5771(15)	255(16)
F(6A)	2504(14)	1916(12)	6118(16)	206(13)

* Equivalent isotropic U defined as one third of the trace of the orthogonalized U_{ij} tensor

Table 2. Bond lengths (Å) for

Ir(1)-Cl(1)	2.455 (3)
Ir(1)-P(1)	2.381 (4)
Ir(1)-P(2)	2.345 (4)
Ir(1)-P(3)	2.394 (4)
Ir(1)-S(1)	2.369 (4)
Ir(1)-C(1)	1.959 (10)
P(1)-C(11)	1.814 (14)
P(1)-C(12)	1.793 (16)
P(1)-C(13)	1.812 (18)
P(2)-C(21)	1.832 (15)
P(2)-C(22)	1.806 (19)
P(2)-C(23)	1.777 (14)
P(3)-C(31)	1.824 (15)
P(3)-C(32)	1.813 (16)
P(3)-C(33)	1.808 (18)
S(1)-C(3)	1.703 (13)
C(1)-N(1)	1.321 (15)
N(1)-C(2)	1.446 (18)
N(1)-C(101)	1.473 (12)
C(2)-C(3)	1.344 (18)
C(101)-N(1A)	1.506 (17)
Ir(2)-Cl(1A)	2.452 (5)
Ir(2)-P(1A)	2.373 (4)
Ir(2)-P(2A)	2.341 (4)
Ir(2)-P(3A)	2.369 (5)
Ir(2)-S(1A)	2.393 (4)

Ir(2)-C(1A)	1.985 (12)
P(1A)-C(11A)	1.795 (15)
P(1A)-C(12A)	1.775 (21)
P(1A)-C(13A)	1.787 (19)
P(2A)-C(21A)	1.803 (17)
P(2A)-C(22A)	1.809 (18)
P(2A)-C(23A)	1.815 (19)
P(3A)-C(31A)	1.785 (16)
P(3A)-C(32A)	1.754 (20)
P(3A)-C(33A)	1.799 (23)
S(1A)-C(3A)	1.704 (16)
C(1A)-N(1A)	1.325 (15)
N(1A)-C(2A)	1.426 (18)
C(2A)-C(3A)	1.359 (23)
P(4)-F(1)	1.592 (15)
P(4)-F(2)	1.581 (13)
P(4)-F(3)	1.566 (13)
P(4)-F(4)	1.522 (18)
P(4)-F(5)	1.539 (12)
P(4)-F(6)	1.570 (14)
P(4A)-F(1A)	1.510 (13)
P(4A)-F(2A)	1.572 (14)
P(4A)-F(3A)	1.510 (14)
P(4A)-F(4A)	1.564 (13)
P(4A)-F(5A)	1.492 (19)
P(4A)-F(6A)	1.498 (20)



Table 3. Bond angles (°) for

Cl(1)-Ir(1)-P(1)	91.9(1)
Cl(1)-Ir(1)-P(2)	83.7(1)
P(1)-Ir(1)-P(2)	93.8(1)
Cl(1)-Ir(1)-P(3)	92.1(1)
P(1)-Ir(1)-P(3)	172.8(1)
P(2)-Ir(1)-P(3)	92.5(1)
Cl(1)-Ir(1)-S(1)	84.9(1)
P(1)-Ir(1)-S(1)	86.7(1)
P(2)-Ir(1)-S(1)	168.6(1)
P(3)-Ir(1)-S(1)	87.7(1)
Cl(1)-Ir(1)-C(1)	179.3(4)
P(1)-Ir(1)-C(1)	87.5(4)
P(2)-Ir(1)-C(1)	95.9(4)
P(3)-Ir(1)-C(1)	88.6(4)
S(1)-Ir(1)-C(1)	95.5(4)
Ir(1)-P(1)-C(11)	116.4(6)
Ir(1)-P(1)-C(12)	117.3(5)
C(11)-P(1)-C(12)	105.6(8)
Ir(1)-P(1)-C(13)	114.5(6)
C(11)-P(1)-C(13)	101.1(7)
C(12)-P(1)-C(13)	99.5(8)
Ir(1)-P(2)-C(21)	114.8(6)
Ir(1)-P(2)-C(22)	117.0(6)
C(21)-P(2)-C(22)	96.5(7)
Ir(1)-P(2)-C(23)	118.0(6)
C(21)-P(2)-C(23)	103.9(8)
C(22)-P(2)-C(23)	103.7(8)
Ir(1)-P(3)-C(31)	115.9(6)
Ir(1)-P(3)-C(32)	114.8(7)
C(31)-P(3)-C(32)	105.5(8)
Ir(1)-P(3)-C(33)	116.6(7)
C(31)-P(3)-C(33)	101.3(8)
C(32)-P(3)-C(33)	100.6(9)
Ir(1)-S(1)-C(3)	106.9(5)
Ir(1)-C(1)-N(1)	131.3(9)
C(1)-N(1)-C(2)	126.8(9)
C(1)-N(1)-C(101)	120.9(10)
C(2)-N(1)-C(101)	112.3(9)
N(1)-C(2)-C(3)	128.4(12)
S(1)-C(3)-C(2)	130.5(13)
N(1)-C(101)-N(1A)	109.9(9)
Cl(1A)-Ir(2)-P(1A)	86.5(1)
Cl(1A)-Ir(2)-P(2A)	93.8(2)
P(1A)-Ir(2)-P(2A)	91.6(1)
Cl(1A)-Ir(2)-P(3A)	85.0(2)
P(1A)-Ir(2)-P(3A)	170.2(2)
P(2A)-Ir(2)-P(3A)	93.8(2)
Cl(1A)-Ir(2)-S(1A)	85.6(1)
P(1A)-Ir(2)-S(1A)	87.5(1)
mer-(Me ₃ P) ₃ Ir{SCHCHNCH}(Cl)	
P(2A)-Ir(2)-S(1A)	178.9(2)
P(3A)-Ir(2)-S(1A)	87.0(2)

Cl(1A)-Ir(2)-C(1A)	177.9(3)
P(1A)-Ir(2)-C(1A)	94.8(4)
P(2A)-Ir(2)-C(1A)	87.9(3)
P(3A)-Ir(2)-C(1A)	93.6(4)
S(1A)-Ir(2)-C(1A)	92.8(3)
Ir(2)-P(1A)-C(11A)	115.7(7)
Ir(2)-P(1A)-C(12A)	114.7(6)
C(11A)-P(1A)-C(12A)	98.8(8)
Ir(2)-P(1A)-C(13A)	118.8(6)
C(11A)-P(1A)-C(13A)	104.6(9)
C(12A)-P(1A)-C(13A)	101.5(9)
Ir(2)-P(2A)-C(21A)	116.0(7)
Ir(2)-P(2A)-C(22A)	115.8(7)
C(21A)-P(2A)-C(22A)	103.4(9)
Ir(2)-P(2A)-C(23A)	118.0(5)
C(21A)-P(2A)-C(23A)	104.2(8)
C(22A)-P(2A)-C(23A)	96.8(9)
Ir(2)-P(3A)-C(31A)	117.2(6)
Ir(2)-P(3A)-C(32A)	115.8(9)
C(31A)-P(3A)-C(32A)	103.2(10)
Ir(2)-P(3A)-C(33A)	116.7(6)
C(31A)-P(3A)-C(33A)	102.2(9)
C(32A)-P(3A)-C(33A)	99.1(12)
Ir(2)-S(1A)-C(3A)	105.1(5)
Ir(2)-C(1A)-N(1A)	129.0(9)
C(101)-N(1A)-C(1A)	119.4(10)
C(101)-N(1A)-C(2A)	111.6(10)
C(1A)-N(1A)-C(2A)	129.0(12)
N(1A)-C(2A)-C(3A)	125.1(13)
S(1A)-C(3A)-C(2A)	130.4(12)
F(1)-P(4)-F(2)	90.0(8)
F(1)-P(4)-F(3)	176.5(8)
F(2)-P(4)-F(3)	89.2(7)
F(1)-P(4)-F(4)	89.1(9)
F(2)-P(4)-F(4)	176.1(8)
F(3)-P(4)-F(4)	91.9(8)
F(1)-P(4)-F(5)	88.1(8)
F(2)-P(4)-F(5)	92.0(8)
F(3)-P(4)-F(5)	88.6(7)
F(4)-P(4)-F(5)	91.7(9)
F(1)-P(4)-F(6)	92.2(9)
F(2)-P(4)-F(6)	85.3(9)
F(3)-P(4)-F(6)	91.1(9)
F(4)-P(4)-F(6)	90.9(10)
F(5)-P(4)-F(6)	177.3(10)
F(1A)-P(4A)-F(2A)	90.6(8)
F(1A)-P(4A)-F(3A)	179.5(11)
Table 3. (cont)	
F(2A)-P(4A)-F(3A)	89.8(10)
F(1A)-P(4A)-F(4A)	87.7(8)
F(2A)-P(4A)-F(4A)	174.1(10)
F(3A)-P(4A)-F(4A)	91.8(10)
F(1A)-P(4A)-F(5A)	86.7(11)
F(2A)-P(4A)-F(5A)	93.8(13)

F(3A)-P(4A)-F(5A)	93.5(14)
F(4A)-P(4A)-F(5A)	91.8(13)
F(1A)-P(4A)-F(6A)	94.2(11)
F(2A)-P(4A)-F(6A)	89.2(10)
F(3A)-P(4A)-F(6A)	85.6(14)
F(4A)-P(4A)-F(6A)	85.2(10)
F(5A)-P(4A)-F(6A)	176.8(12)

Table 4. Anisotropic displacement coefficients ($\text{\AA}^2 \times 10^3$) for mer-(Me₃P)₃Ir{SCHCHNCH}(Cl)

	U ₁₁	U ₂₂	U ₃₃	U ₁₂	U ₁₃	U ₂₃
Ir(1)	33(1)	26(1)	38(1)	3(1)	8(1)	9(1)
Cl(1)	43(2)	41(2)	74(2)	-3(2)	-1(2)	8(2)
P(1)	49(2)	56(2)	40(2)	3(2)	14(2)	-3(2)
P(2)	58(2)	31(2)	52(2)	13(2)	8(2)	15(2)
P(3)	53(2)	37(2)	65(2)	9(2)	30(2)	13(2)
S(1)	46(2)	44(2)	63(2)	0(2)	-7(2)	24(2)
C(1)	44(8)	29(7)	34(7)	5(6)	14(6)	5(5)
N(1)	38(6)	26(6)	36(6)	2(4)	10(4)	7(4)
C(2)	70(11)	24(7)	83(11)	7(7)	21(9)	31(7)
C(3)	38(8)	52(9)	76(10)	-3(7)	-9(8)	26(8)
C(11)	76(12)	83(12)	66(11)	-5(9)	24(9)	-18(9)
C(12)	57(10)	67(10)	70(11)	10(8)	25(8)	-13(8)
C(13)	67(11)	91(12)	61(10)	-1(9)	35(8)	12(9)
C(21)	75(12)	41(9)	99(13)	23(8)	12(9)	15(8)
C(22)	85(13)	59(11)	139(16)	16(9)	55(12)	62(11)
C(23)	75(11)	70(11)	66(11)	17(9)	2(8)	23(9)
C(31)	62(11)	74(11)	111(14)	23(9)	49(10)	34(10)
C(32)	139(18)	84(13)	75(13)	30(12)	56(12)	5(10)
C(33)	110(14)	55(10)	148(17)	47(10)	89(13)	42(11)
C(101)	40(8)	30(7)	45(8)	0(6)	11(6)	14(6)
Ir(2)	33(1)	32(1)	43(1)	5(1)	12(1)	9(1)
Cl(1A)	64(3)	77(3)	95(3)	20(2)	48(2)	43(2)
P(1A)	38(2)	65(3)	56(2)	15(2)	9(2)	16(2)
P(2A)	50(2)	31(2)	98(3)	-4(2)	28(2)	-7(2)
P(3A)	54(3)	86(3)	65(3)	22(2)	15(2)	41(2)
S(1A)	104(3)	46(2)	47(2)	14(2)	30(2)	1(2)
C(1A)	46(8)	23(7)	27(6)	-2(5)	-1(5)	-1(5)
N(1A)	38(6)	31(6)	42(6)	8(5)	7(5)	11(5)
C(2A)	63(10)	28(7)	83(11)	19(7)	19(8)	12(7)
C(3A)	53(9)	33(8)	74(11)	9(7)	18(8)	-5(7)
C(11A)	47(11)	76(13)	174(21)	3(9)	-5(11)	5(13)
C(12A)	70(12)	127(17)	100(14)	54(12)	24(10)	38(13)
C(13A)	74(12)	109(14)	65(11)	24(11)	1(9)	30(10)
C(21A)	77(13)	30(8)	203(22)	-1(8)	66(14)	3(11)
C(22A)	98(15)	89(14)	94(14)	5(11)	33(11)	-27(11)
C(23A)	90(13)	45(9)	121(15)	20(9)	50(11)	3(10)
C(31A)	45(10)	90(13)	109(14)	8(9)	8(9)	57(11)
C(32A)	168(24)	244(33)	79(16)	124(24)	14(15)	46(18)
C(33A)	70(13)	134(19)	202(24)	32(13)	48(14)	119(18)
P(4)	82(3)	81(3)	60(3)	49(3)	12(2)	10(2)
F(1)	166(12)	238(16)	99(9)	114(12)	67(8)	87(10)
F(2)	92(8)	168(12)	157(11)	79(8)	19(7)	77(9)
F(3)	93(8)	138(10)	93(8)	25(7)	29(6)	53(7)
F(4)	143(12)	321(22)	200(15)	172(15)	76(11)	158(16)
F(5)	194(14)	97(9)	130(11)	-29(9)	60(10)	-5(8)
Table 4. (cont)						
F(6)	279(22)	108(11)	211(17)	82(13)	5(15)	-58(11)
P(4A)	81(3)	78(3)	67(3)	32(3)	26(2)	24(2)
F(1A)	208(15)	112(10)	100(10)	32(10)	5(9)	31(8)

F(2A)	312(21)	77(9)	173(14)	98(11)	69(13)	40(9)
F(3A)	460(35)	210(19)	69(10)	95(21)	12(14)	39(11)
F(4A)	245(17)	65(8)	182(14)	-40(9)	40(12)	30(8)
F(5A)	86(11)	439(35)	292(24)	133(16)	54(13)	129(23)
F(6A)	187(15)	148(13)	400(28)	104(12)	212(19)	137(16)

The anisotropic displacement exponent takes the form: $-2p^2(h^2a^2U_{11} + \dots + 2hka^*b^*U_{12})$

Table 5. H-Atom coordinates ($\times 10^4$) and isotropic displacement coefficients ($\text{\AA}^2 \times 10^3$) for
mer-(Me₃P)₃Ir{SCHCHNCH}(Cl)

	x	y	z	U
H(1A)	2531	6183	6927	80
H(2A)	3150	3681	7825	80
H(3A)	4611	4316	8949	80
H(11A)	3501	8602	10539	80
H(11B)	4640	8361	10462	80
H(11C)	4178	9142	9911	80
H(12A)	1634	7822	9239	80
H(12B)	2045	8266	8434	80
H(12C)	1521	7073	8292	80
H(13A)	2500	6605	10162	80
H(13B)	2476	5798	9274	80
H(13C)	3569	6234	10047	80
H(21A)	3636	10051	7600	80
H(21B)	3274	9399	8311	80
H(21C)	4527	9870	8398	80
H(22A)	4593	9450	6350	80
H(22B)	5553	9282	7097	80
H(22C)	5005	8420	6199	80
H(23A)	2532	8608	6108	80
H(23B)	2620	7445	5912	80
H(23C)	2021	7831	6670	80
H(31A)	7008	7064	6543	80
H(31B)	6537	8018	6878	80
H(31C)	7141	7477	7604	80
H(32A)	5062	5956	5362	80
H(32B)	3955	5644	5667	80
H(32C)	4399	6796	5588	80
H(33A)	6163	5132	6582	80
H(33B)	6239	5368	7650	80
H(33C)	5132	4731	6962	80
H(10A)	1938	3692	6416	80
H(10B)	1426	4651	6355	80
H(1AA)	1143	2479	7053	80
H(2AA)	671	5350	7538	80
H(3AA)	-43	5349	8766	80
H(11D)	-3588	1483	6355	80
H(11E)	-2722	799	6328	80
H(11F)	-3163	1036	7222	80
H(12D)	-3191	3315	7371	80
H(12E)	-2748	2938	8276	80
H(12F)	-2053	3917	8034	80
H(13D)	-2464	3115	5885	80
H(13E)	-1266	3727	6416	80
H(13F)	-1461	2630	5774	80
Table 5. (cont)				
H(21D)	-1291	-1093	6686	80

H(21E)	-1097	-644	7749	80
H(21F)	-2027	-380	7039	80
H(22D)	-771	-5	5449	80
H(22E)	-1456	815	5680	80
H(22F)	-212	1188	5674	80
H(23D)	753	-436	6540	80
H(23E)	1425	726	6830	80
H(23F)	1224	87	7591	80
H(31D)	3111	2076	9462	80
H(31E)	2585	1769	8394	80
H(31F)	2792	2924	8924	80
H(32D)	2051	2484	10721	80
H(32E)	1586	3360	10318	80
H(32F)	783	2427	10526	80
H(33D)	1757	613	9875	80
H(33E)	471	432	9632	80
H(33F)	1083	167	8850	80

VITA

The author was born at Ellis Hospital in Schenectady, New York, on May 7, 1968 to Leon and Esther Grieb. He graduated from Burnt Hills-Ballston Lake High School in the summer of 1986. The following August he started his college education at Hartwick College in Oneonta, New York where he received his B.S. in Biochemistry in the spring of 1990. Following the summer, he entered graduate school at Virginia Tech. Arthur eventually joined Dr. Merola's group where he started working towards his Master's degree in Chemistry.